

CBD: A Certified Backdoor Detector Based on Local Dominant Probability

Zhen Xiang Zidi Xiong Bo Li
University of Illinois Urbana-Champaign
{zxiangaa, zidix2, lbo}@illinois.edu

Abstract

Backdoor attack is a common threat to deep neural networks. During testing, samples embedded with a backdoor trigger will be misclassified as an adversarial target by a backdoored model, while samples without the backdoor trigger will be correctly classified. In this paper, we present the first *certified backdoor detector* (CBD), which is based on a novel, adjustable conformal prediction scheme based on our proposed statistic *local dominant probability*. For any classifier under inspection, CBD provides 1) a detection inference, 2) the condition under which the attacks are guaranteed to be detectable for the same classification domain, and 3) a probabilistic upper bound for the false positive rate. Our theoretical results show that attacks with triggers that are more resilient to test-time noise and have smaller perturbation magnitudes are more likely to be detected with guarantees. Moreover, we conduct extensive experiments on four benchmark datasets considering various backdoor types, such as BadNet, CB, and Blend. CBD achieves comparable or even higher detection accuracy than state-of-the-art detectors, and it in addition provides detection certification. Notably, for backdoor attacks with random perturbation triggers bounded by $\ell_2 \leq 0.75$ which achieves more than 90% attack success rate, CBD achieves 100% (98%), 100% (84%), 98% (98%), and 72% (40%) empirical (certified) detection true positive rates on the four benchmark datasets GTSRB, SVHN, CIFAR-10, and TinyImageNet, respectively, with low false positive rates.

1 Introduction

Despite the success of deep neural networks (DNNs) in many applications, they are vulnerable to adversarial attacks such as backdoor attacks [46, 36]. A DNN being backdoored will learn to predict an adversarial target class for test samples embedded with a backdoor trigger, while maintaining a high accuracy on clean test samples without the trigger [18, 8, 42, 65, 50, 43, 51, 37].

Backdoor detection is a popular task for backdoor defense. It aims to detect if a given model is backdoored without access to the training set or any real test samples that are possibly embedded with the trigger [48, 64]. The task corresponds to practical scenarios where the user of an app or a legacy system containing a DNN seeks to know if the model is backdoor attacked, where the training set is not available [1]. Various empirical approaches have been proposed for backdoor detection, most of which are based on trigger reverse engineering [67, 6, 75, 69, 56, 62, 24], or meta classification [82, 29]. However, none of these works quantitatively investigate the conditions under which the backdoor attacks are guaranteed to be detectable. Without a detection guarantee, DNNs are still vulnerable to future attacks (e.g.) with new trigger types [51, 87, 70].

In this paper, we make the first attempt toward the *certification* of backdoor detection. Certification is an important concept for studies on the robustness of DNNs against adversarial examples [61, 17, 52, 7, 45]. In particular, a robustness certification refers to a probabilistic or deterministic guarantee for a model to produce desired outputs (e.g. correct label prediction) when the adversarial perturbation applied to the inputs satisfies certain conditions (e.g. with some constrained perturbation magnitude) [33, 58, 32, 10, 59]. As an analogy, we propose a *certified backdoor detector* (CBD)

that is guaranteed to trigger an alarm if the attack for a given domain satisfies certain conditions. In Sec. 3, we introduce the detection procedure of CBD based on conformal prediction (with our proposed, optional adjustment scheme) using a novel (model-level) statistic named *local dominant probability*. The calibration set for conformal prediction is obtained from a small number of benign shadow models trained on a small validation set, which addresses the unavailability of the training set. In Sec. 4, we derive the condition for attacks with detection guarantee, as well as a probabilistic upper bound for the false positive rate of our detector, for any prescribed significance level specifying the aggressiveness of the detection. Notably, our certification is comprehensive – for any domain, more effective attacks with strong *trigger robustness* (which measures the resilience of a trigger against test-time noises) and more stealthy attacks (against human inspectors) with small trigger perturbation magnitudes are easier to be detected with guarantees. Moreover, both our detector and the certification method do not assume the trigger incorporation mechanism or the training configuration of the model, which allows their potential application to future attacks. Our contributions are summarized below:

- We propose CBD, the first certified backdoor detector, which is based on an adjustable conformal prediction scheme using a novel *local dominant probability* statistic.
- We propose a certification method and show that for any domain, backdoor attacks with stronger *trigger robustness* and smaller trigger perturbation magnitudes are more likely to be detected by CBD with guarantee. We also derive a probabilistic upper bound for the false positive rate of CBD.
- We show that CBD achieves comparable or even higher detection accuracy than state-of-the-art detectors against three types of backdoors. We also show that for backdoor attacks with random perturbation triggers bounded by $\ell_2 \leq 0.75$, CBD achieves 100% (98%), 100% (84%), 98% (98%), and 72% (40%) empirical (certified) true positive rates on GTSRB, SVHN, CIFAR-10, and TinyImageNet, respectively, with only 0%, 0%, 6%, and 10% false positive rates, respectively.

2 Related Work

Backdoor Detection Methods Existing methods for backdoor detection are all empirical without theoretical guarantees. An important type of reverse-engineering-based method estimates putative triggers for anomaly detection [67, 6, 75, 41, 78, 73, 79, 76, 69, 56, 62, 24]. Certification for these methods is hard due to the complexity of trigger reverse engineering. Another type of detector is based on meta-classification that involves a large number of shadow models trained with and without attacks [82, 29]. Differently, our CBD is based on conformal prediction involving a scalar detection statistic (rather than a high dimensional feature vector employed by [82, 29]), such that only a small number of benign shadow models will be required. More importantly, our CBD is certified, i.e. with a detection guarantee, which is different from all the detection methods mentioned above.

Other Backdoor Defense Tasks Backdoor defenses during training aim to produce a backdoor-free classifier from the possibly poisoned training set [63, 5, 74, 14, 25, 57, 77, 23, 4, 16]. These defenses require access to the training set, which is unavailable for backdoor detection. Backdoor mitigation aims to “repair” models being backdoor attacked [40, 72, 35, 19, 88, 85], which can be viewed as a downstream task following backdoor detection. Inference-stage trigger detection aims to detect if a test sample contains the trigger [15, 55, 12, 9, 44, 34]. However, backdoor detection is performed before the inference stage, where test samples are not available. These defense tasks will not be further discussed due to their fundamental differences from the backdoor detection task.

Certified Backdoor Defenses Existing methods mostly modify the training process to prevent the backdoor from being learned, while manipulating the test sample to destroy any potentially embedded triggers [86, 71, 27, 53]. These methods are not applicable to the backdoor detection problem where both the training set and the test samples are not available. More importantly, all these existing certified defenses are deployed during training, which requires an uncontaminated training process fully controlled by the defender. In contrast, in this paper, we consider a stronger threat model that allows the attacker to have full control of the training process.

3 Detection Method

3.1 Problem Definition

Threat Model Consider a classification domain with sample space \mathcal{X} and label space \mathcal{Y} . A backdoor attack is specified by a trigger with some incorporation function $\delta : \mathcal{X} \rightarrow \mathcal{X}$ and a target class $t \in \mathcal{Y}$. For a successful backdoor attack, the victim classifier will predict to the target class t whenever a

test sample is embedded with the trigger, while test samples without the trigger will be correctly classified [18, 8, 42, 38]. In this paper, we do allow advanced attackers with full control of the training process [51, 87, 70, 50, 3]. This is deemed a stronger threat model than all previous works on certified backdoor defense where the defender is assumed with full control of the training process. However, in this paper, we do not consider backdoor attacks with multiple triggers or target classes [84, 83] – even empirical detection of these attacks is a challenging problem [80].

Goal of Certified Backdoor Detection The fundamental goal is backdoor detection, i.e. to infer if a given classifier $f(\cdot; w) : \mathcal{X} \rightarrow \mathcal{Y}$ is backdoored or not [48, 64]. The defender has no access to the training set or any test samples that may contain the trigger. In practice, the defender also has no access to benign classifiers with high accuracy for the same domain as $f(\cdot; w)$ – otherwise, these benign classifiers can be used for the task, and detection will be unnecessary. However, the defender is assumed with a small validation set of clean samples for detection – this is a standard assumption made by most post-training backdoor defenses [67, 82, 75, 56, 41].

Beyond model inference, a *certified* backdoor detector also needs to provide each classification domain (associated with the model to be inspected) with a condition on δ , t , and w , such that any successful backdoor attack with a trigger δ and a target class t on a victim classifier $f(\cdot; w)$ (trained on this classification domain) is guaranteed to be detected if the condition is satisfied. The stronger a certification is, the more likely a successful attack on the domain will be detectable with guarantee. Moreover, a certification has to be associated with a guarantee on the false positive rate; otherwise, an arbitrarily strong certification can be achieved by increasing the aggressiveness of the detection rule.

3.2 Overview of CBD Detection

Key Intuition For a successful backdoor attack with a trigger δ and a target class t , a test instance x embedded with the trigger (denoted by $\delta(x)$) will be classified to the target class t with high probability. Practical backdoor triggers should also be robust (i.e. resilient) to noises either from the environment or introduced by simple defenses based on input-preprocessing such as blurring and/or quantization [81, 39]. Such *trigger robustness* can be measured by the distribution of the model prediction in the neighborhood of each $\delta(x)$ – the more robust the trigger is, the more samples in the neighborhood of $\delta(x)$ will be predicted to the target class t . Thus, if the perturbation magnitude of a robust trigger, i.e. $\|\delta(x) - x\|_2$, is small (which is usual for backdoor attacks to achieve stealthiness), a significant proportion of samples in the neighborhood of x will also be classified to class t due to their closeness to $\delta(x)$. Such an increment in the target class probability in the neighborhood of all instances is captured by our proposed statistic named *local dominant probability* (LDP) to distinguish backdoored classifiers from benign ones – the former tend to have a larger LDP than the latter.

Outline of CBD Detection Procedure In short, CBD performs an *adjustable* conformal prediction to test if the LDP statistic computed for the model to be inspected is sufficiently large to trigger an alarm. A small number of shadow models (with the same architecture as the model to be inspected) are trained on a relatively small validation set, with an LDP computed for each shadow model to form a calibration set. Then, a small proportion of outliers with large values in the calibration set are optionally removed, e.g., by anomaly detection. Based on this adjusted calibration set, the p-value is computed for the LDP for the model to be inspected. The model is deemed to be backdoored if the p-value is less than some prescribed significance level (e.g. the classical 0.05 for statistical testing).

3.3 Definition of LDP

We first define a *samplewise local probability vector* (SLPV) to represent the distribution of the model prediction outcomes in the neighborhood of any given sample. Then, based on SLPV, we define the *samplewise trigger robustness* (STR) that measures the resilience of a trigger to the Gaussian noise when it is embedded in a particular sample. Finally, we define the LDP statistic based on SLPV.

Definition 3.1. (Samplewise Local Probability Vector (SLPV)) For any classifier $f(\cdot; w) : \mathcal{X} \rightarrow \mathcal{Y}$ with parameters w , the SLPV for any input $x \in \mathcal{X}$ is a probability vector $\mathbf{p}(x|w, \sigma) \in [0, 1]^K$ over the $K = |\mathcal{Y}|$ classes, with the k -th entry defined by $p_k(x|w, \sigma) \triangleq \mathbb{P}_{\epsilon \sim \mathcal{N}(0, \sigma^2 I)}(f(x + \epsilon; w) = k)$, $\forall k \in \mathcal{Y}$, where $\mathcal{N}(\mu, \Sigma)$ represents Gaussian distribution with mean μ and covariance Σ .

Remarks: If $f(\cdot; w)$ is continuous at x with $f(x; w) = k$ for some $k \in \mathcal{Y}$, it is trivial to show that $p_k(x|w, \sigma) \rightarrow 1$ as $\sigma \rightarrow 0$, i.e. the SLPV becomes a singleton at the predicted class of x without the Gaussian noise. In practice, SLPV can be estimated by Monte Carlo for any given model and sample.



(a) Benign classifier with a small LDP close to $\frac{1}{4}$. (b) Classifier being backdoored with a large LDP.

Figure 1: Illustration of the difference in LDP between benign and backdoored classifiers on a classification domain with $K = 4$ classes. A backdoor attack with a robust trigger δ (with a small perturbation magnitude) and a target class 4 (with orange decision region) changes the class distribution in the neighborhood of x_1 , x_2 , and x_3 , resulting in a larger LDP for the backdoored model than for the benign model.

Definition 3.2. (Samplewise Trigger Robustness (STR)) Consider a backdoor attack with a trigger δ and a target class $t \in \mathcal{Y}$ against a victim model $f(\cdot; w)$. For any sample $x \in \mathcal{X}$ and any isotropic Gaussian distribution $\mathcal{N}(0, \sigma^2 I)$, the STR is defined by the t -th entry of the SLPV for $\delta(x)$ (i.e. sample x with the trigger δ embedded), which is denoted by $R_{\delta,t}(x|w, \sigma) \triangleq p_t(\delta(x)|w, \sigma)$.

Remarks: STR measures the resilience of a trigger against Gaussian noises. Usually, strong STR can be naturally achieved by embedding the trigger in a large variety of samples during training.

Definition 3.3. (Local Dominant Probability (LDP)) Consider a domain with $K = |\mathcal{Y}|$ classes and an isotropic Gaussian distribution $\mathcal{N}(0, \sigma^2 I)$. The LDP for a classifier $f(\cdot; w)$ is defined by

$$s(w) = \left\| \frac{1}{K} \sum_{k=1}^K p(x_k|w, \sigma) \right\|_{\infty} \quad (1)$$

where x_1, \dots, x_K are K independent random samples satisfying $f(x_k; w) = k, \forall k \in \{1, \dots, K\}$.

Remarks: By the definition, LDP for a given classifier $f(\cdot; w)$ is computed on x_1, \dots, x_K independently sampled from the K classes respectively, satisfying $f(x_k; w) = k$ for $\forall k$. LDP computed on more samples per class yields similar detection and certification performance empirically. Specifically, we first compute the SLPV for each of the K samples. Then we take the average of the K SLPVs and pick the maximum entry as the LDP for $f(\cdot; w)$. Note that LDP is always no less than $\frac{1}{K}$.

As stated in the key intuitions in Sec. 3.2, LDP tends to be larger for backdoored classifiers than for benign ones. This can be understood from the illustration in Fig. 1 for a classification domain with $K = 4$ classes. For the benign classifier on the left, the SLPVs for x_1, \dots, x_4 are almost orthogonal to each other, leading to a small LDP close to $\frac{1}{4}$. On the right, we consider a backdoor attack with a robust trigger δ and a target class 4 (with orange decision region). The strong STRs for x_1 , x_2 , and x_3 (represented by the large orange regions around $\delta(x_1)$, $\delta(x_2)$, and $\delta(x_3)$), together with the small trigger perturbation magnitudes (i.e. small $\|\delta(x_i) - x_i\|_2$ for $i = 1, 2, 3$), significantly change the class distribution in the neighborhood of each of x_1 , x_2 , and x_3 . In particular, there will be a clear increment in the 4-th entry of the SLPVs for x_1 , x_2 , and x_3 . Thus, the 4-th entry associated with the backdoor target class will dominate the average SLPV over x_1, \dots, x_4 , leading to a large LDP.

3.4 CBD Detection Procedure

Although backdoored and benign classifiers have different LDP distributions, it is still a challenge in practice to set a detection threshold. To solve this problem, we propose to use the conformal prediction, which employs a calibration set for supervision [66, 2]. Here, the calibration set consists of LDP statistics obtained from a small number of benign shadow models trained on the small validation set possessed by the defender. However, the actual benign classifiers to be inspected are usually trained on more abundant data, such that the LDPs for these classifiers will likely follow a different distribution from the LDPs for the shadow models without sufficient training. In particular, the LDPs in the calibration set (obtained from the shadow models) may easily have an overly large sample variance and a heavy tail of large outliers. Directly using this calibration set for conformal prediction may lead to a conservative detection due to an overly large detection threshold.

Thus, we propose an optional adjustment scheme that treats the m largest LDP statistics in the calibration set as outliers. In practice, prior knowledge may be required to determine the exact value

of m , while in our experiments, a small m/N (≤ 0.2 , where N is the size of the calibration set) may significantly increase the detection or certification power of our CBD with only small increment to the false positive rate. The detection procedure of our CBD consists of the following four steps:

- 1) Given a classifier $f(\cdot; w)$ to be inspected, estimate LDP $s(w)$ based on Def. 3.3.
- 2) Train (benign) shadow models $f(\cdot; w_1), \dots, f(\cdot; w_N)$ on the clean validation dataset, and construct a calibration set $\mathcal{S}_N = \{s(w_1), \dots, s(w_N)\}$ by computing the LDP for each model.
- 3) Compute the adjusted conformal p-value (assuming m large outliers) defined by:

$$q_m(w) = 1 - \frac{1 + \min\{|\{s \in \mathcal{S}_N : s < s(w)\}|, N - m\}}{N - m + 1} \quad (2)$$

- 4) Trigger an alarm if $q_m(w) \leq \alpha$, where α is a prescribed significance level (e.g. $\alpha=0.05$).

4 CBD Certification

In addition to a detection inference, CBD also provides a certification, which is a condition under which attacks are guaranteed to be detectable. Detailed proofs in this section are shown in App. A.

Theorem 4.1. (Backdoor Detection Guarantee) *For an arbitrary classifier $f(\cdot; w) : \mathcal{X} \rightarrow \mathcal{Y}$ to be inspected, let x_1, \dots, x_K be the K randomly selected samples and $\mathcal{N}(0, \sigma^2 I)$ be the isotropic Gaussian distribution used to compute the LDP for $f(\cdot; w)$. Let α be the prescribed significance level of CBD. A backdoor attack with a trigger δ and a target class t is guaranteed to be detected if:*

$$\Delta < \sigma(\Phi^{-1}(1 - s_{(N-m-\lfloor \alpha(N-m+1) \rfloor)}) - \Phi^{-1}(1 - \pi)) \quad (3)$$

where Φ is the standard Gaussian CDF, $\pi = \min_{k=1, \dots, K} R_{\delta, t}(x_k | w, \sigma)$ is the minimum STR over x_1, \dots, x_K , $\Delta = \max_{k=1, \dots, K} \|\delta(x_k) - x_k\|_2$ is the maximum perturbation magnitude of the trigger, m is the number of assumed outliers in the calibration set \mathcal{S}_N with size N , and $s_{(n)}$ denotes the n -th smallest element in \mathcal{S}_N .

Proof (sketch). The STR for each sample x_k equals the t -th entry of the SLPV for $\delta(x_k)$ by Def. 3.2. We also connect the SLPV for $\delta(x_k)$ to the SLPV for x_k using the Neyman-Pearson lemma ([49]). Based on this connection, we derive the lower bound for the minimum STR, such that the t -th entry of the SLPV of each x_k is sufficiently large to result in a large LDP for the attack to be detected. \square

Remarks: (1) **(Main Results)** For fixed trigger perturbation size (Δ), detection of attacks with larger STR (π) is more likely to be guaranteed; while for fixed STR, detection of attacks with smaller trigger perturbation size is more likely to be guaranteed. (2) Our backdoor detection guarantee is inspired by the randomized smoothing approach in [10] for certified robustness against adversarial examples. However, certified backdoor detection and certified robustness against adversarial examples are fundamentally different, as will be detailed in App. I. (3) Certified backdoor detection and certified robustness against backdoors complement each other. The former provides detection guarantees to strong backdoor attacks, while the latter prevents the trigger from being learned during training [86, 53]. The two types of certification may cover the entire attack space together in the future, such that a backdoor attack will be either strong enough to be detected or weak enough to be disabled.

A meaningful certification for backdoor detection should also be along with a guarantee for the false positive rate (FPR). Otherwise, one can easily design a backdoor detector that always triggers an alarm, which provides detection guarantees to all backdoor attacks but is useless in practice.

Theorem 4.2. (Probabilistic Upper Bound for FPR) *Consider a random calibration set $\mathcal{S}_N = \{s_1, \dots, s_N\}$ with s_1, \dots, s_N i.i.d. following some continuous distribution F . Consider a random benign classifier $f(\cdot; W)$ with LDP $s(W)$ following some distribution \bar{F} . Assume F dominates \bar{F} in the sense of first-order stochastic dominance. Let m be any number of assumed outliers in \mathcal{S}_N and let α be any prescribed significance level of CBD. Then, the FPR of CBD on $f(\cdot; W)$ conditioned on \mathcal{S}_N , which is denoted by $Z_N = \mathbb{P}(q_m(W) \leq \alpha | \mathcal{S}_N)$ based on Eq. (2), will be first-order dominated by a random variable B following $\text{Beta}(m + l + 1, N - m - l)$ with $l = \lfloor \alpha(N - m + 1) \rfloor$, i.e. $B \succeq_1 Z_N$. In other words, $\mathbb{P}(Z_N \leq q) \geq \mathbb{P}(B \leq q)$ for any real q .*

Proof (sketch). We first express the false positive rate Z_N in terms of the order statistics on the elements of the random calibration set \mathcal{S}_N . Then, we derive the lower bound of the CDF of Z_N using the distribution of order statistics followed by a binomial expansion. \square

Remarks: The assumption that F dominates \tilde{F} in Thm. 4.2 generally holds in practice. Again, this is because the actual benign classifiers to be inspected are usually trained on more abundant data than the benign shadow models. Empirical results supporting this assumption are shown in Sec. 5.4. Moreover, an analysis of this phenomenon is presented in App. B, where we show on binary Bayes classifiers that a higher empirical loss can easily lead to a larger expected LDP.

While we have shown that Z_N conditioned on a random calibration set of size N is upper bounded by a Beta random variable in the sense of first-order stochastic dominance, in Col. 4.3 below, we show that asymptotically, the upper bound of Z_N converges to a constant in probability as $N \rightarrow \infty$.

Corollary 4.3. (Asymptotic Property of FPR) *Consider the settings in Thm. 4.2. For any $\xi > 0$, $\lim_{N \rightarrow +\infty} \mathbb{P}(Z_N \leq \tau) = 1$, where $\tau = \alpha + (1 - \alpha)\beta + \xi$ with $\beta = m/N$.*

Proof (sketch). We show that any random variable B with the Beta distribution described in Thm. 4.2 satisfies $\lim_{N \rightarrow +\infty} \mathbb{P}(B \leq \tau) = 1$. Then, the corollary is proved since Z_N is dominated by B . \square

Remarks: For classical conformal prediction without adjustment where $m = 0$, we will have $\beta = 0$ and $\lim_{N \rightarrow +\infty} \mathbb{P}(Z_N \leq \alpha + \xi) = 1$ for any $\xi > 0$. In this case, the upper bound of the false positive rate of our CBD converges to the prescribed significance level α in probability.

5 Experiment

There have been many different types of backdoor attacks proposed, each also with a wide range of configurations. Thus, it is infeasible to evaluate our CBD over the entire space of backdoor attacks. Inspired by the evaluation protocol for certified robustness [10], in Sec. 5.1, we focus on backdoor attacks with random perturbation triggers to comprehensively evaluate the certification capability of our CBD. In Sec. 5.2, we compare CBD with three state-of-the-art backdoor detectors (all “uncertified”) against backdoor attacks with three popular trigger types to evaluate the detection capability of CBD. In Sec. 5.3, we present ablation studies (e.g. on the number of shadow models used by CBD). Additional results and other supportive empirical analyses are shown in Sec. 5.4.

5.1 Evaluation of CBD Certification

For certified robustness, the prediction of a test example is unchanged with a guarantee, if the magnitude of the adversarial perturbation is smaller than the *certified radius* [10]. Certified robustness is usually evaluated by the *certified accuracy* on some random test set as the proportion of the samples that are guaranteed to be correctly classified if the magnitude of the adversarial perturbation is no larger than some prescribed value. As an analog, our certification for backdoor detection is specified by an inequality that involves both the STR and the perturbation magnitude of the trigger, which naturally produces a two-dimensional “*certified region*” (illustrated in Fig. 7 and Fig. 8 in Apdx. D). Our certification method is evaluated on a set of random backdoor attacks, each using a random pattern as the trigger, with the perturbation magnitude satisfying some ℓ_2 constraint. We are interested in the proportion of the attacks falling into the certified region, i.e. guaranteed to be detected.

5.1.1 Setup

Dataset: Our experiments are conducted on four benchmark image datasets, GTSRB [60], SVHN [47], CIFAR-10 [30], and TinyImageNet [11], following their standard train-test splits. Due to the large number of models that will be trained to evaluate our certification method, except for GTSRB, we use 40% of the training set to train these models. We also reserve 5,000 samples from the test set of GTSRB, SVHN, and CIFAR-10, and 10,000 samples from the test set of TinyImageNet (much smaller than the training size for the models for evaluation) for the defender to train the shadow models. More details about these datasets are deferred to App. C.1.

Evaluation Metric: Following the convention, the detection performance of CBD is evaluated by the true positive rate (TPR) defined by the proportion of attacks being detected (with a correct inference of the target class) and the false positive rate (FPR) defined by the proportion of benign classifiers falsely detected. For certification, we define certified TPR (CTPR) as the proportion of a set of attacks that are guaranteed to be detectable, i.e. falling into the certified region.

Attack Setting: For each dataset, we create 50 backdoor attacks, each with a randomly selected target class. For each attack, we generate a random trigger, which is a random perturbation embedded

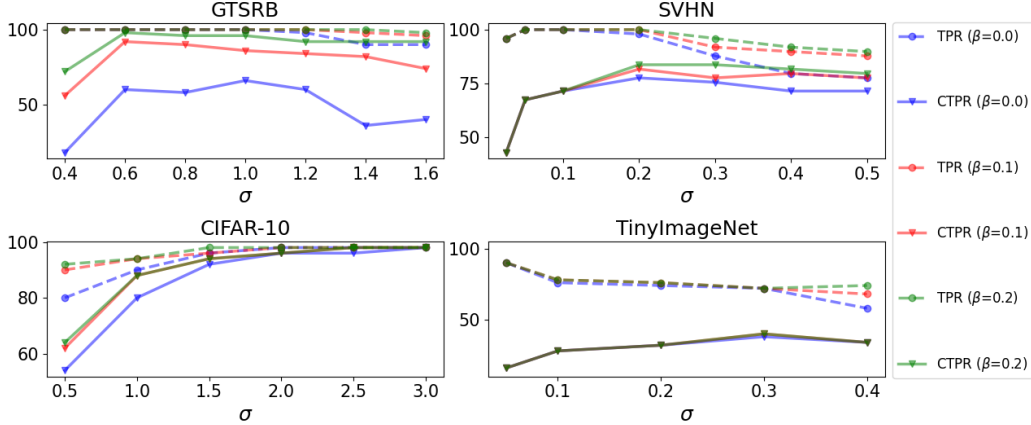


Figure 2: Certification performance of CBD against backdoor attacks with random triggers with perturbation magnitude $\ell_2 \leq 0.75$ measured by CTPR (solid) for a range of σ for $\beta = 0, 0.1, 0.2$. The CTPRs are all upper-bounded by the TPRs (dashed), showing the correctness of our certification. Notably, CBD achieves up to 98% (100%), 84% (100%), 98% (98%), and 40% (72%) CTPRs (TPRs) on GTSRB, SVHN, CIFAR-10, and TinyImageNet, respectively, across all choices of σ and β . An increment in β , the assumed ratio of calibration outliers, may lead to further increments in both CTPR and TPR. The hyperparameter σ can be determined using the calibration set in practice.

by $\delta(x) = x + v$ with $\|v\|_2 \leq 0.75$. The generation process also involves random nullification of the trigger pattern, which helps the trigger to be learned. More details about trigger generation are deferred to App. C.2 due to space limitations. The poisoning ratios for the attacks on GTSRB, SVHN, CIFAR-10, and TinyImageNet are 7.8%, 15.3%, 11.3%, and 12.4%, respectively. Lower poisoning ratios may largely reduce the attack success rate since many randomly generated triggers are relatively hard to learn. Results for triggers with larger perturbation size are shown in App. D.

Training: For model architecture, we use the winning model on the leaderboard [31] for GTSRB, MobileNetV2 [54] for SVHN, the same architecture in [82] for CIFAR-10, and ResNet-34 [22] for TinyImageNet. For each dataset, 50 benign models are trained (also on the 40% training set except for GTSRB) to evaluate the FPR. The accuracies for these benign models are roughly 98%, 92%, 78%, and 47% on GTSRB, SVHN, CIFAR-10, and TinyImageNet, respectively. For each attack, we train a model with $\geq 90\%$ attack success rate and $\leq 2\%$ degradation in the benign accuracy (or re-generate the attack for training until both conditions are satisfied). More details about the training configurations are shown in App. C.3. Finally, we train 100 shadow models for each of GTSRB, SVHN, and CIFAR-10, and 50 shadow models for TinyImageNet using the same architectures and configurations as above – these shadow models are used by our CBD for detection and certification.

5.1.2 Certification Performance

In Fig. 2, we show the CTPR (solid) of our CBD against the attacks with the random perturbation trigger on the four datasets for a range of σ and for $\beta = m/N \in \{0, 0.1, 0.2\}$. The TPR (dashed) for each combination of σ and β is also plotted for reference. Recall that β here represents the proportion of assumed outliers in the calibration set for the adjustment of the conformal prediction, and σ is the standard deviation of the isotropic Gaussian distribution for the LDP computation. In our experiments, 1024 random Gaussian noises are generated for each sample used to compute the LDP. The significance level for conformal prediction is set to the classical $\alpha = 0.05$ for statistical testing.

In general, our certification is effective, which covers up to 98%, 84%, and 98% backdoor attacks with the random perturbation trigger (all achieved with $\beta = 0.2$) on GTSRB, SVHN, and CIFAR-10, respectively. Even for the very challenging TinyImageNet dataset, CBD certifies up to 40% of these attacks. Moreover, for all choices of β and σ , CTPR is upper-bounded by TPR. For example, for the aforementioned CTPRs on the four datasets, the corresponding TPRs are 100%, 100%, 98%, and 72%, respectively (with FPRs 0%, 0%, 6%, and 10%, respectively, see App. D). In fact, all attacks with the detection guarantee are detected empirically, showing the correctness of our certification.

We also make the following observations regarding the hyperparameters β and σ : 1) An increment in β may lead to an increment in both CTPR and TPR. This is due to the existence of a heavy tail

(corresponding to large outliers) in the LDP distribution for the calibration set. While an overly large β may cause a significant increment to FPR, our additional results in App. D show that empirically, this is not the case for $\beta \leq 0.2$. 2) Each domain has its own proper range for the choice of σ . In general, the detection power of CBD (reflected by TPR) reduces as σ becomes overly small. This phenomenon agrees with our remarks on Def. 3.1 – SLPV converges to a singleton at the labeled class as σ approaches zero, regardless of the presence of a backdoor attack. Moreover, the certification power (reflected by CTPR) also reduces for small σ 's, which matches the inequality (3) in Thm. 4.1. For overly large σ 's, on the other hand, LDP for benign classifiers may also grow and possibly approach one, resulting in a large FPR. However, in this case, LDP is no longer computed in a truly 'local' context, contrary to the intuition implied by its name. In Sec. 5.2, we will introduce a practical scheme to choose a proper σ for each domain based on the shadow models.

5.2 Evaluation of CBD Detection

Here, we show the detection performance of CBD against backdoor attacks with various trigger types, including the BadNet square [18], the "chessboard" (CB) pattern [75], and the blended pattern [8]. For each of GTSRB, SVHN, and CIFAR-10, we train 20 models (using the full training set) for each trigger type following the same training configurations described in Sec. 5.1.1. TinyImageNet is not considered here due to the high training cost. Details for each trigger type and attack settings are shown in App. C.4. We also compare CBD with three state-of-the-art backdoor detectors without certification, which are Neural Cleanse (NC) [67], K-Arm [56], and MNTD [82]. In particular, K-Arm and MNTD require manual selection of the detection threshold. For both of them, we choose the threshold that maximizes the TPR while keeping a 5% FPR for each dataset. Moreover, we devise a "supervised" version of CBD, named CBD_{sup} , which still uses LDP as the detection statistic but without the conformal prediction. The detection threshold for CBD_{sup} is determined in the same way as for K-Arm and MNTD, i.e. by maximizing the TPR with a controlled 5% FPR.

In practice, CBD needs to choose a moderately large σ for each detection task. To this end, we first initialize a small σ such that for each of the N shadow models, the SLPVs for the K samples used for computing the LDP all concentrate at the labeled classes. In this case, the LDPs for all the shadow models are close to $\frac{1}{K}$. Then, we gradually increase σ until $\frac{1}{N \times K} \sum_{n=1}^N \sum_{k=1}^K p_k(x_k^{(n)} | w_n, \sigma) < \psi$ for some relatively small ψ , where $x_k^{(n)}$ is the k -th sample for LDP computation for the n -th model, i.e. the SLPVs are no longer concentrated at the labeled classes. In the left of Fig. 4, we show the choice of σ based on the above scheme for a range of ψ , which exhibits a trend of convergence as ψ decreases. We also notice that σ selected for $\psi < 0.2$ roughly matches the σ choices in Fig. 2 that yields relatively high CTPR and TPR, showing the effectiveness of our scheme. In our evaluation of CBD detection, we set $\psi = 0.1$, which yields $\sigma = 1.15, 0.39, 1.14$ for GTSRB, SVHN, and CIFAR-10, respectively. Other choices of σ for ψ less than 0.2 yield similar detection performance.

As shown in Tab. 1, CBD achieves comparable or even higher TPRs than the SOTA detectors (that benefit from unrealistic supervision) for all trigger types on all datasets. CBD also provides non-trivial detection guarantees to most attack types on these datasets. The relatively low CTPRs, e.g. for BadNet on GTSRB, are due to the large perturbation magnitude of the trigger. The even better TPRs achieved by CBD_{sup} , though with the same supervision as for the SOTA detectors, show the effectiveness of the LDP statistic in distinguishing backdoored models from benign ones. Such effectiveness is further verified by the receiver operating characteristic (ROC) curves for CBD_{sup} . Compared with the baseline detectors, CBD_{sup} achieves generally higher overall areas under curves (AUCs) across the three datasets.

5.3 Ablation Study

We show that the time efficiency and data efficiency of CBD can be improved by training fewer shadow models and using fewer samples for training the shadow models, respectively, without significant degradation in the detection or certification performance. In particular, we show in Tab. 2 that CBD with $\beta = 0.2$ achieves similar TPRs and CTPRs for the same set of attacks in Sec. 5.2 when we reduce the number of shadow models from 100 to 50, 25, and 10, respectively. Such robustness of CBD to the calibration size further verifies the clear separation between the benign and backdoored classifiers using our proposed LDP. In Tab. 3, we show that with shadow models trained on only 100

Table 1: Certified detection of CBD for $\beta = 0, 0.1, 0.2$ (shaded), with the empirical detection performance (measured by TPR (%)) compared with NC, K-Arm, MNTD, and CBD_{sup} against BadNet, CB, and Blend attacks on GTSRB, SVHN, and CIFAR-10. The parentheses in each shaded cell contain the CTPR (%) associated with the TPR outside the parentheses. CBD achieves comparable or even higher empirical TPRs compared with the SOTA baselines and provides non-trivial (or even tight) certification for different attacks and datasets. FPRs (%) are reported on benign classifiers.

	GTSRB				SVHN				CIFAR-10				Average TPR
	benign	BadNet	CB	Blend	benign	BadNet	CB	Blend	benign	BadNet	CB	Blend	
NC	20	50	75	20	40	80	100	95	20	35	95	60	67.8
K-Arm	5	100	100	100	5	100	70	40	5	100	80	55	82.8
MNTD	5	20	0	0	5	10	10	15	5	90	100	75	35.6
CBD_{sup}	5	100	95	100	5	100	100	90	5	65	100	55	89.4
CBD_0	0	75 (5)	95 (80)	80 (20)	0	75 (45)	100 (100)	80 (75)	0	50 (5)	100 (90)	45 (30)	77.2
$\text{CBD}_{0.1}$	0	90 (15)	95 (85)	90 (25)	0	90 (55)	100 (100)	80 (80)	20	75 (20)	100 (95)	55 (35)	86.1
$\text{CBD}_{0.2}$	0	90 (15)	95 (85)	95 (35)	0	95 (65)	100 (100)	90 (80)	25	75 (25)	100 (100)	60 (40)	88.9

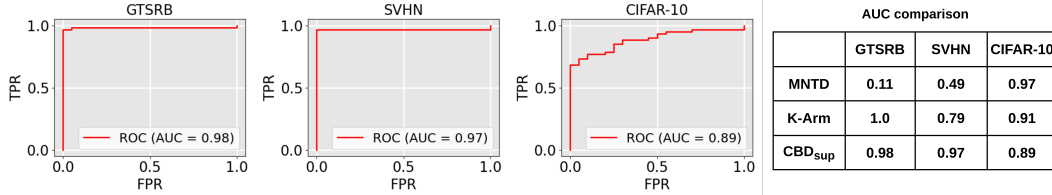


Figure 3: Receiver operating characteristic (ROC) curves of CBD_{sup} aggregated over all three trigger types on GTSRB, SVHN, and CIFAR-10, respectively. CBD_{sup} with our proposed LDP statistic achieves higher overall areas under curves (AUCs) than K-Arm and MNTD across the three datasets.

Table 2: Certified detection of CBD (with CTPR inside the parentheses and TPR outside) for $\beta = 0.2$ using 10, 25, 50, and 100 (the default in Sec. 5.2) shadow models. Both the detection and certification performance of CBD are not significantly affected by reducing the number of shadow models.

# shadow	GTSRB				SVHN				CIFAR-10			
	benign	BadNet	CB	Blend	benign	BadNet	CB	Blend	benign	BadNet	CB	Blend
10	0	95 (10)	95 (85)	95 (35)	0	75 (45)	100 (100)	90 (75)	25	85 (25)	100 (100)	55 (40)
25	0	95 (5)	95 (85)	95 (25)	0	95 (45)	100 (100)	80 (75)	25	80 (25)	100 (100)	70 (40)
50	0	95 (15)	95 (85)	95 (40)	0	95 (65)	100 (100)	85 (75)	25	80 (25)	100 (100)	60 (40)
100	0	90 (15)	95 (85)	95 (35)	0	95 (65)	100 (100)	90 (80)	25	75 (25)	100 (100)	60 (40)

Table 3: Certified detection of CBD (with CTPR inside the parentheses and TPR outside) for $\beta = 0.2$ and $\beta = 0.4$, respectively, with 100 shadow models trained on fewer samples (100 per class) than the default settings in Sec. 5.2. Due to the significantly insufficient training of the shadow models, a larger β is needed to maintain a similar level of TPR and CTPR as in Sec. 5.2.

	GTSRB				SVHN				CIFAR-10			
	benign	BadNet	CB	Blend	benign	BadNet	CB	Blend	benign	BadNet	CB	Blend
$\text{CBD}_{0.2}$	0	90 (5)	95 (85)	90 (25)	0	75 (45)	100 (95)	80 (75)	0	35 (0)	95 (90)	45 (40)
$\text{CBD}_{0.4}$	0	95 (5)	95 (85)	95 (35)	0	95 (45)	100 (100)	85 (75)	5	60 (10)	100 (95)	55 (40)

clean samples per class, CBD requires a larger β to achieve similar TPRs and CTPRs. This is because more shadow models will exhibit an abnormally large LDP due to significantly insufficient training.

5.4 Additional Experiments

Empirical validation of the stochastic dominance assumption in Thm. 4.2. In the middle of Fig. 4, we show the histograms (with the associated empirical CDF) of the LDP statistics for the shadow models and the benign models for all four datasets. The statistics for each dataset are obtained using the practically selected σ . The LDP for the benign models is clearly dominated by the LDP for the shadow models in the sense of first-order stochastic dominance.

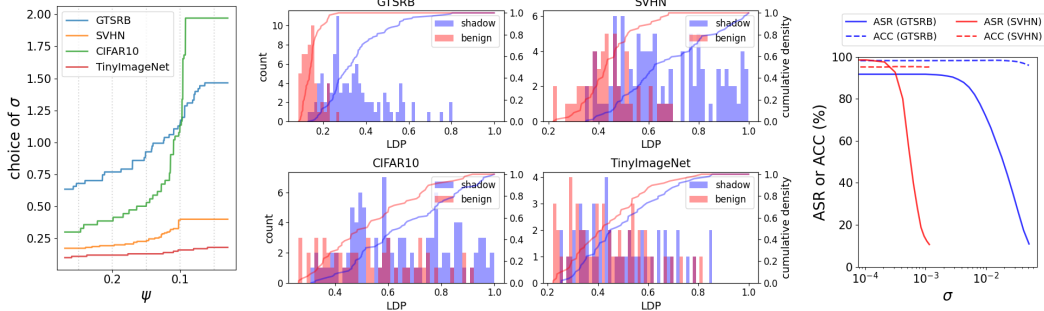


Figure 4: Supportive results: **(Left)** Choice of σ for a range of ψ based on our selection scheme, which matches the σ choices in Fig. 2 with high CTPR and TPR. **(Middle)** The histograms of the LDP statistics for the shadow models and the benign models, with the associated empirical CDFs. LDP for benign models is stochastically dominated by the LDP for shadow models for all datasets. **(Right)** Vulnerability of WaNet attack on GTSRB and SVHN. Attack success rate (ASR) reduces with a negligible drop in benign accuracy (ACC) when inputs are smoothed by Gaussian noise.

Class imbalance is not the reason for a large LDP. In our experiments involving generally balanced datasets, backdoor poisoning (i.e. embedding the trigger in a large variety of samples during training) not only enhances the trigger robustness of the attack, but also introduces an imbalance in the poisoned training set. Thus, it is important to show that the large LDPs observed in our experiments are a result of the robustness of the trigger, rather than the class imbalance. Note that if class imbalance can also cause a large LDP, there will easily be false alarms for benign classifiers trained on imbalanced datasets¹. Here, we train two groups of benign models on SVHN, with 20 models per group. For the first group, the models are trained on a balanced dataset with 3,000 images per class. For each model in the second group, the training set contains 4,400 additional images labeled to some randomly selected class. With the same model architecture and training configurations, the two groups have similar LDP distributions, with mean \pm std being 0.445 ± 0.125 and 0.429 ± 0.119 , respectively, and with a 0.698 p-value for the t-test for mean. Thus, LDP will not be affected by class imbalance in general, and our method indeed detects the backdoor attack rather than the class imbalance.

Advanced attacks. Based on the key ideas in Sec. 1, CBD requires the attack to have a large STR over the sample distribution. However, this requirement is not always satisfied, especially for some advanced attacks with subtle, sample-specific triggers, such as WaNet [51]. Although not detectable or certifiable by our CBD, these attacks can hardly survive noises either from the environment or simple preprocessing-based defenses in practice. To see this, for each of GTSRB and SVHN, we train 20 models with successful WaNet attacks. We consider a simple test-time defense by applying 1024 randomly sampled Gaussian noises from distribution $\mathcal{N}(0, \sigma^2 I)$ to each input and then performing a majority vote. As shown in the right of Fig. 4, for both datasets and for small σ , the average attack success rate (ASR) quickly drops without clear scarifies in the benign accuracy (ACC).

6 Conclusion

In this paper, we proposed CBD, the first certified backdoor detector, which is based on an adjustable conformal prediction using a novel LDP statistic. CBD not only performs detection inference but also provides a condition for attacks that are guaranteed to be detectable. Our theoretical results show that backdoor attacks with a trigger more resilient to noises and with a smaller perturbation magnitude are more likely to be detected with a guarantee. Our empirical results show the strong certification and detection performance of CBD on four benchmark datasets. In future research, we aim to enhance the certification bound to encompass backdoor attacks with larger trigger perturbation norms, such as rotational triggers and subject-based triggers.

Acknowledgements This work is partially supported by the National Science Foundation under grant No. 1910100, No. 2046726, No. 2229876, DARPA GARD, the National Aeronautics and Space Administration (NASA) under grant no. 80NSSC20M0229, Alfred P. Sloan Fellowship, and the Amazon research award.

¹This is the case for the backdoor detector in [68] which leverages the overfitting to the backdoor trigger during training – benign classifiers trained on imbalanced datasets will also easily trigger a (false) detection.

References

- [1] Model Zoo. <https://modelzoo.co/>.
- [2] Anastasios N. Angelopoulos and Stephen Bates. A gentle introduction to conformal prediction and distribution-free uncertainty quantification, 2021.
- [3] Hamed Pirsiavash Aniruddha Saha, Akshayvarun Subramanya. Hidden trigger backdoor attacks. In *AAAI Conference on Artificial Intelligence (AAAI)*, 2020.
- [4] Eitan Borgnia, Jonas Geiping, Valeriia Cherepanova, Liam Fowl, Arjun Gupta, Amin Ghiasi, Furong Huang, Micah Goldblum, and Tom Goldstein. DP-InstaHide: Provably Defusing Poisoning and Backdoor Attacks with Differentially Private Data Augmentations. In *ICLR Workshop on Security and Safety in Machine Learning Systems*, March 2021.
- [5] Bryant Chen, Wilka Carvalho, Nathalie Baracaldo, Heiko Ludwig, Benjamin Edwards, Taesung Lee, Ian Molloy, and Biplav Srivastava. Detecting backdoor attacks on deep neural networks by activation clustering. <http://arxiv.org/abs/1811.03728>, Nov 2018.
- [6] Huili Chen, Cheng Fu, Jishen Zhao, and Farinaz Koushanfar. DeepInspect: A black-box trojan detection and mitigation framework for deep neural networks. In *International Joint Conference on Artificial Intelligence (IJCAI)*, pages 4658–4664, 7 2019.
- [7] Pin-Yu Chen, Huan Zhang, Yash Sharma, Jinfeng Yi, and Cho-Jui Hsieh. Zoo: Zeroth order optimization based black-box attacks to deep neural networks without training substitute models. In *ACM Workshop on Artificial Intelligence and Security (AISec)*, page 15–26, 2017.
- [8] Xinyun Chen, Chang Liu, Bo Li, Kimberly Lu, and Dawn Song. Targeted backdoor attacks on deep learning systems using data poisoning. <https://arxiv.org/abs/1712.05526v1>, 2017.
- [9] Edward Chou, Florian Tramèr, and Giancarlo Pellegrino. Sentinet: Detecting localized universal attacks against deep learning systems. In *2020 IEEE Security and Privacy Workshops (SPW)*, pages 48–54. IEEE, 2020.
- [10] Jeremy Cohen, Elan Rosenfeld, and Zico Kolter. Certified adversarial robustness via randomized smoothing. In *Proceedings of the 36th International Conference on Machine Learning*, pages 1310–1320, 2019.
- [11] Jia Deng, Wei Dong, Richard Socher, Li-Jia Li, Kai Li, and Li Fei-Fei. Imagenet: A large-scale hierarchical image database. In *IEEE Conference on Computer Vision and Pattern Recognition (CVPR)*, pages 248–255, 2009.
- [12] Bao Gia Doan, Ehsan Abbasnejad, and Damith C. Ranasinghe. Februus: Input purification defense against trojan attacks on deep neural network systems. In *Annual Computer Security Applications Conference (ACSAC)*, page 897–912, 2020.
- [13] Yinpeng Dong, Xiao Yang, Zhijie Deng, Tianyu Pang, Zihao Xiao, Hang Su, and Jun Zhu. Black-box detection of backdoor attacks with limited information and data. In *Proceedings of the IEEE/CVF International Conference on Computer Vision (ICCV)*, 2021.
- [14] Min Du, Ruoxi Jia, and Dawn Song. Robust anomaly detection and backdoor attack detection via differential privacy. In *International Conference on Learning Representations (ICLR)*, 2020.
- [15] Yansong Gao, Change Xu, Derui Wang, Shiping Chen, Damith C. Ranasinghe, and Surya Nepal. STRIP: A defence against trojan attacks on deep neural networks. In *Annual Computer Security Applications Conference (ACSAC)*, 2019.
- [16] Jonas Geiping, Liam Fowl, Gowthami Somepalli, Micah Goldblum, Michael Moeller, and Tom Goldstein. What doesn’t kill you makes you robust(er): Adversarial training against poisons and backdoors. In *ICLR 2021 Workshop on Security and Safety in Machine Learning Systems*, 2021.
- [17] Ian J. Goodfellow, Jonathon Shlens, and Christian Szegedy. Explaining and harnessing adversarial examples. In *International Conference on Learning Representations (ICLR)*, 2015.

- [18] Tianyu Gu, Kang Liu, Brendan Dolan-Gavitt, and Siddharth Garg. Badnets: Evaluating backdooring attacks on deep neural networks. *IEEE Access*, 7:47230–47244, 2019.
- [19] Jiyang Guan, Zhuozhuo Tu, Ran He, and Dacheng Tao. Few-shot backdoor defense using shapley estimation. In *CVPR*, 2022.
- [20] Wenbo Guo, Lun Wang, Xinyu Xing, Min Du, and Dawn Song. Tabor: A highly accurate approach to inspecting and restoring Trojan backdoors in AI systems. <https://arxiv.org/abs/1908.01763>, 2019.
- [21] Frank R. Hampel. The influence curve and its role in robust estimation. *Journal of the American Statistical Association*, 69, 1974.
- [22] Kaiming He, Xiangyu Zhang, Shaoqing Ren, and Jian Sun. Deep residual learning for image recognition. In *IEEE Conference on Computer Vision and Pattern Recognition (CVPR)*, 2016.
- [23] Sanghyun Hong, Varun Chandrasekaran, Yiğitcan Kaya, Tudor Dumitras, and Nicolas Papernot. On the effectiveness of mitigating data poisoning attacks with gradient shaping. <https://arxiv.org/abs/2002.11497>, 2020.
- [24] Xiaoling Hu, Xiao Lin, Michael Cogswell, Yi Yao, Susmit Jha, and Chao Chen. Trigger hunting with a topological prior for trojan detection. In *International Conference on Learning Representations*, 2022.
- [25] Kunzhe Huang, Yiming Li, Baoyuan Wu, Zhan Qin, and Kui Ren. Backdoor defense via decoupling the training process. In *International Conference on Learning Representations (ICLR)*, 2022.
- [26] Andrew Ilyas, Sung Min Park, Logan Engstrom, Guillaume Leclerc, and Aleksander Madry. Datamodels: Predicting predictions from training data, 2022.
- [27] Jinyuan Jia, Yupei Liu, Xiaoyu Cao, and Neil Zhenqiang Gong. Certified robustness of nearest neighbors against data poisoning and backdoor attacks. In *AAAI Conference on Artificial Intelligence*, 2020.
- [28] Diederik P. Kingma and Jimmy Ba. Adam: A method for stochastic optimization. In *International Conference on Learning Representations (ICLR)*, 2015.
- [29] Soheil Kolouri, Aniruddha Saha, Hamed Pirsiavash, and Heiko Hoffmann. Universal litmus patterns: Revealing backdoor attacks in cnns. In *IEEE/CVF Conference on Computer Vision and Pattern Recognition (CVPR)*, pages 298–307, 2020.
- [30] Alex Krizhevsky. Learning multiple layers of features from tiny images. *University of Toronto*, 05 2012.
- [31] Leaderboard. GTSRB Leaderboard. <https://www.kaggle.com/c/nyu-cv-fall-2018/leaderboard>, 2018.
- [32] Mathias Lecuyer, Vaggelis Atlidakis, Roxana Geambasu, Daniel Hsu, and Suman Jana. Certified robustness to adversarial examples with differential privacy. In *2019 IEEE Symposium on Security and Privacy (SP)*, 2019.
- [33] Linyi Li, Tao Xie, and Bo Li. SoK: Certified Robustness for Deep Neural Networks. In *44th IEEE Symposium on Security and Privacy*, San Francisco, CA, 2023.
- [34] Xi Li, Zhen Xiang, David J. Miller, and George Kesidis. Test-time detection of backdoor triggers for poisoned deep neural networks. In *ICASSP 2022 - 2022 IEEE International Conference on Acoustics, Speech and Signal Processing (ICASSP)*, 2022.
- [35] Yige Li, Xixiang Lyu, Nodens Koren, Lingjuan Lyu, Bo Li, and Xingjun Ma. Neural Attention Distillation: Erasing Backdoor Triggers from Deep Neural Networks. In *International Conference on Learning Representations (ICLR)*, 2021.
- [36] Yiming Li, Yong Jiang, Zhifeng Li, and Shu-Tao Xia. Backdoor learning: A survey. *IEEE Transactions on Neural Networks and Learning Systems*, pages 1–18, 2022.

- [37] Yuezun Li, Yiming Li, Baoyuan Wu, Longkang Li, Ran He, and Siwei Lyu. Invisible backdoor attack with sample-specific triggers. In *IEEE International Conference on Computer Vision (ICCV)*, 2021.
- [38] Cong Liao, Haoti Zhong, Anna Squicciarini, Sencun Zhu, and David Miller. Backdoor embedding in convolutional neural network models via invisible perturbation. In *CODASPY*, 2020.
- [39] Ji Lin, Chuang Gan, and Song Han. Defensive quantization: When efficiency meets robustness. In *International Conference on Learning Representations (ICLR)*, 2019.
- [40] Kang Liu, Brendan Dolan-Gavitt, and Siddharth Garg. Fine-pruning: Defending against backdoor attacks on deep neural networks. In *International Symposium on Research in Attacks, Intrusions, and Defenses (RAID)*, 2018.
- [41] Yingqi Liu, Wen-Chuan Lee, Guanhong Tao, Shiqing Ma, Yousra Aafer, and Xiangyu Zhang. ABS: Scanning neural networks for back-doors by artificial brain stimulation. In *ACM SIGSAC Conference on Computer and Communications Security (CCS)*, page 1265–1282, 2019.
- [42] Yingqi Liu, Shiqing Ma, Yousra Aafer, Wen-Chuan Lee, Juan Zhai, Weihang Wang, and Xiangyu Zhang. Trojaning attack on neural networks. In *Network and Distributed System Security (NDSS) Symposium*, San Diego, CA, 2018.
- [43] Yunfei Liu, Xingjun Ma, James Bailey, and Feng Lu. Reflection Backdoor: A Natural Backdoor Attack on Deep Neural Networks. In *European Conference on Computer Vision (ECCV)*, 2020.
- [44] Wanlun Ma, Derui Wang, Ruoxi Sun, Minhui Xue, Sheng Wen, and Yang Xiang. The “beatrice” resurrections: Robust backdoor detection via gram matrices. *arXiv preprint arXiv:2209.11715*, 2022.
- [45] Aleksander Madry, Aleksandar Makelov, Ludwig Schmidt, Dimitris Tsipras, and Adrian Vladu. Towards deep learning models resistant to adversarial attacks. In *International Conference on Learning Representations (ICLR)*, 2018.
- [46] David J. Miller, Zhen Xiang, and George Kesidis. Adversarial learning in statistical classification: A comprehensive review of defenses against attacks. *Proceedings of the IEEE*, 108:402–433, 2020.
- [47] Yuval Netzer, Tao Wang, Adam Coates, Alessandro Bissacco, Bo Wu, and Andrew Y. Ng. Reading digits in natural images with unsupervised feature learning. In *NIPS Workshop on Deep Learning and Unsupervised Feature Learning 2011*, 2011.
- [48] NeurIPS. Trojan Detection Challenge NeurIPS 2022. <https://trojandetection.ai/>, 2022.
- [49] Jerzy Neyman and Egon S. Pearson. On the problem of the most efficient tests of statistical hypotheses. *Philosophical Transactions of the Royal Society of London. Series A, Containing Papers of a Mathematical or Physical Character*, 231:289–337, 1933.
- [50] Anh Nguyen and Anh Tran. Input-aware dynamic backdoor attack. In *Proceedings of Advances in Neural Information Processing Systems (NeurIPS)*, 2020.
- [51] Anh Nguyen and Anh Tran. Wanet - imperceptible warping-based backdoor attack. In *International Conference on Learning Representations (ICLR)*, 2021.
- [52] David Wagner Nicholas Carlini. Towards evaluating the robustness of neural networks. In *IEEE Symposium on Security and Privacy (SP)*, pages 39–57, May 2017.
- [53] Elan Rosenfeld, Ezra Winston, Pradeep Ravikumar, and J. Zico Kolter. Certified robustness to label-flipping attacks via randomized smoothing. In *Proceedings of the 37th International Conference on Machine Learning*, 2020.
- [54] Mark Sandler, Andrew Howard, Menglong Zhu, Andrey Zhmoginov, and Liang-Chieh Chen. Inverted residuals and linear bottlenecks: Mobile networks for classification, detection and segmentation. In *IEEE Conference on Computer Vision and Pattern Recognition (CVPR)*, 2018.

- [55] Esha Sarkar, Yousif Alkindi, and Michail Maniatakos. Backdoor suppression in neural networks using input fuzzing and majority voting. *IEEE Design & Test*, 37(2):103–110, 2020.
- [56] Guangyu Shen, Yingqi Liu, Guanhong Tao, Shengwei An, Qiuling Xu, Siyuan Cheng, Shiqing Ma, and Xiangyu Zhang. Backdoor Scanning for Deep Neural Networks through K-Arm Optimization. In *International Conference on Machine Learning (ICML)*, 2021.
- [57] Yanyao Shen and Sujay Sanghavi. Learning with bad training data via iterative trimmed loss minimization. In *International Conference on Machine Learning (ICML)*, pages 5739–5748, 2019.
- [58] Gagandeep Singh, Timon Gehr, Matthew Mirman, Markus Püschel, and Martin Vechev. Fast and effective robustness certification. In *Advances in Neural Information Processing Systems*, 2018.
- [59] Gagandeep Singh, Timon Gehr, Markus Püschel, and Martin Vechev. Robustness certification with refinement. In *International Conference on Learning Representations*, 2019.
- [60] Johannes Stalldkamp, Marc Schlipsing, Jan Salmen, and Christian Igel. Man vs. computer: Benchmarking machine learning algorithms for traffic sign recognition. *Neural Networks*, 32:323–332, 2012.
- [61] Christian Szegedy, Wojciech Zaremba, Ilya Sutskever, Joan Bruna, Dumitru Erhan, Ian Goodfellow, and Rob Fergus. Intriguing properties of neural networks. In *International Conference on Learning Representations (International Conference on Learning Representations (ICLR))*, 2014.
- [62] Guanhong Tao, Guangyu Shen, Yingqi Liu, Shengwei An, Qiuling Xu, Shiqing Ma, Pan Li, and Xiangyu Zhang. Better trigger inversion optimization in backdoor scanning. In *2022 Conference on Computer Vision and Pattern Recognition (CVPR 2022)*, 2022.
- [63] Brandon Tran, Jerry Li, and Aleksander Madry. Spectral signatures in backdoor attacks. In *Advances in Neural Information Processing Systems (NIPS)*, 2018.
- [64] IARPA TrojAI: Trojans in artificial intelligence. <https://www.iarpa.gov/index.php/research-programs/trojai/trojai-baa>, 2019.
- [65] Alexander Turner, Dimitris Tsipras, and Aleksander Madry. Clean-label backdoor attacks. <https://people.csail.mit.edu/madry/lab/cleanlabel.pdf>, 2019.
- [66] Vladimir Vovk. Conditional validity of inductive conformal predictors. In *Proceedings of the Asian Conference on Machine Learning*, pages 475–490, 04–06 Nov 2012.
- [67] Bolun Wang, Yuanshun Yao, Shawn Shan, Huiying Li, Bimal Viswanath, Haitao Zheng, and Ben Y. Zhao. Neural cleanse: Identifying and mitigating backdoor attacks in neural networks. In *IEEE Symposium on Security and Privacy (SP)*, 2019.
- [68] Hang Wang, Zhen Xiang, David J Miller, and George Kesidis. Mm-bd: Post-training detection of backdoor attacks with arbitrary backdoor pattern types using a maximum margin statistic. In *2024 IEEE Symposium on Security and Privacy (SP)*, 2024.
- [69] Ren Wang, Gaoyuan Zhang, Sijia Liu, Pin-Yu Chen, Jinjun Xiong, and Meng Wang. Practical detection of trojan neural networks: Data-limited and data-free cases. In *European Conference on Computer Vision (ECCV)*, 2020.
- [70] Zhenting Wang, Juan Zhai, and Shiqing Ma. Bppattack: Stealthy and efficient trojan attacks against deep neural networks via image quantization and contrastive adversarial learning. In *IEEE Conference on Computer Vision and Pattern Recognition (CVPR)*, 2022.
- [71] Maurice Weber, Xiaojun Xu, Bojan Karlaš, Ce Zhang, and Bo Li. Rab: Provable robustness against backdoor attacks. In *2023 IEEE Symposium on Security and Privacy (SP)*, pages 640–657, 2023.
- [72] Dongxian Wu and Yisen Wang. Adversarial neuron pruning purifies backdoored deep models. In *NeurIPS*, 2021.

- [73] Zhen Xiang, David J. Miller, Siheng Chen, Xi Li, and George Kesidis. Detecting backdoor attacks against point cloud classifiers. In *IEEE International Conference on Acoustics, Speech and Signal Processing (ICASSP)*, 2022.
- [74] Zhen Xiang, David J. Miller, and George Kesidis. A benchmark study of backdoor data poisoning defenses for deep neural network classifiers and a novel defense. In *IEEE MLSP*, Pittsburgh, 2019.
- [75] Zhen Xiang, David J. Miller, and George Kesidis. Detection of backdoors in trained classifiers without access to the training set. *IEEE Transactions on Neural Networks and Learning Systems*, pages 1–15, 2020.
- [76] Zhen Xiang, David J. Miller, and George Kesidis. L-RED: Efficient post-training detection of imperceptible backdoor attacks without access to the training set. In *IEEE International Conference on Acoustics, Speech and Signal Processing (ICASSP)*, pages 3745–3749, 2021.
- [77] Zhen Xiang, David J. Miller, and George Kesidis. Reverse engineering imperceptible backdoor attacks on deep neural networks for detection and training set cleansing. *Computers and Security*, 106, 2021.
- [78] Zhen Xiang, David J. Miller, and George Kesidis. Post-training detection of backdoor attacks for two-class and multi-attack scenarios. In *International Conference on Learning Representations (ICLR)*, 2022.
- [79] Zhen Xiang, David J. Miller, Hang Wang, and George Kesidis. Detecting scene-plausible perceptible backdoors in trained DNNs without access to the training set. *Neural Computation*, 33(5):1329–1371, 2021.
- [80] Zhen Xiang, Zidi Xiong, and Bo Li. Umd: Unsupervised model detection for x2x backdoor attacks. In *Proceedings of the 40th International Conference on Machine Learning*, 2023.
- [81] Weilin Xu, David Evans, and Yanjun Qi. Feature squeezing: Detecting adversarial examples in deep neural networks. In *Network and Distributed System Security (NDSS) Symposium*, 2018.
- [82] Xiaojun Xu, Qi Wang, Huichen Li, Nikita Borisov, Carl A. Gunter, and Bo Li. Detecting AI Trojans using meta neural analysis. In *IEEE Symposium on Security and Privacy (SP)*, 2021.
- [83] Mingfu Xue, Can He, Jian Wang, and Weiqiang Liu. One-to-n & n-to-one: Two advanced backdoor attacks against deep learning models. *IEEE Transactions on Dependable and Secure Computing*, 19(3):1562–1578, 2022.
- [84] Mingfu Xue, Shifeng Ni, Yinghao Wu, Yushu Zhang, Jian Wang, and Weiqiang Liu. Imperceptible and multi-channel backdoor attack against deep neural networks, 2022.
- [85] Yi Zeng, Si Chen, Won Park, Z. Morley Mao, Ming Jin, and Ruoxi Jia. Adversarial unlearning of backdoors via implicit hypergradient. In *International Conference on Learning Representations (ICLR)*, 2022.
- [86] Yuhao Zhang, Aws Albarghouthi, and Loris D’Antoni. Bagflip: A certified defense against data poisoning. In Alice H. Oh, Alekh Agarwal, Danielle Belgrave, and Kyunghyun Cho, editors, *Advances in Neural Information Processing Systems*, 2022.
- [87] Zhendong Zhao, Xiaojun Chen, Yuexin Xuan, Ye Dong, Dakui Wang, and Kaitai Liang. Defeat: Deep hidden feature backdoor attacks by imperceptible perturbation and latent representation constraints. In *IEEE Conference on Computer Vision and Pattern Recognition (CVPR)*, 2022.
- [88] Runkai Zheng, Rongjun Tang, Jianze Li, and Li Liu. Data-free backdoor removal based on channel lipschitzness. In *ECCV*, 2022.

Ethics Statement

The main purpose of this research is to provide the user of DNN classifiers with a method to detect if the model is backdoor attacked without access to the training set. All attacks used to evaluate our detection method in this paper are created by published backdoor attack strategies on public datasets. Thus, we did not create new threats to society. Moreover, our work provides a new perspective on backdoor defense, as it is the first to address the certification of backdoor detection. It helps other researchers to understand the behavior of deep learning systems facing malicious activities. Code is available at <https://github.com/zhenxianglance/CBD>.

Broader Impacts

While existing backdoor detectors are all empirical [67, 20, 75, 41, 69, 6, 56, 13], our work initiates a new research direction – backdoor detection with certification. Moreover, we first exposed that certified backdoor detectors and certified robustness against backdoor attacks complement each other [86, 71, 27, 53]. Relatively weak attacks, e.g., with a low poisoning rate or a trigger difficult to learn, are more likely to be defeated by robust training strategies with a guarantee. On the other hand, strong backdoor attacks with robustly learned triggers that are resilient to noises are more likely to be detected by our method with a guarantee. We hope that with the development of both branches of certified backdoor defense strategies, future backdoor attacks will be either strong enough to be detected with a guarantee or weak enough to be defeated during training with a guarantee.

Appendix

A Proof of Theorems

A.1 Proof of Thm. 4.1

The proof of Thm. 4.1 is inspired by the proof of Theorem 1 in [10] which leverages the Neyman-Pearson lemma [49]. In particular, we consider the special case of the lemma for isotropic Gaussian distributions as stated in [10].

Lemma A.1. (Neyman-Pearson for Gaussians with Different Means [10]) *Let $X \sim \mathcal{N}(x, \sigma^2 I)$ and $X' \sim \mathcal{N}(x - r, \sigma^2 I)$. Let $h : \mathbb{R}^d \rightarrow \{0, 1\}$ be any deterministic or random function. If $\mathcal{A} = \{z \in \mathbb{R} : r^T z \geq \phi\}$ for some ϕ and $\mathbb{P}(h(X) = 1) \geq \mathbb{P}(X \in \mathcal{A})$, then $\mathbb{P}(h(X') = 1) \geq \mathbb{P}(X' \in \mathcal{A})$.*

Proof of Thm. 4.1. For each $k \in \{1, \dots, K\}$, we defined $r_k = \delta(x_k) - x_k$ for convenience. Also, assume an isotropic Gaussian noise $\epsilon \sim \mathcal{N}(0, \sigma^2 I)$ with standard deviation σ . Then, by the definition of STR in Def. 3.2 and the definition of π as the minimum STR, we have:

$$R_{\delta,t}(x_k|w, \sigma) = \mathbb{P}(f(x_k + r_k + \epsilon; w) = t) \geq \pi$$

Now, we define a half space $\mathcal{A}_k = \{x : r_k^T(x - x_k - r_k) \geq \sigma \|r_k\|_2 \Phi^{-1}(1 - \pi)\}$, such that:

$$\begin{aligned} \mathbb{P}(x_k + r_k + \epsilon \in \mathcal{A}_k) &= \mathbb{P}(r_k^T \epsilon \geq \sigma \|r_k\|_2 \Phi^{-1}(1 - \pi)) \\ &= \mathbb{P}(\sigma \|r_k\|_2 Z \geq \sigma \|r_k\|_2 \Phi^{-1}(1 - \pi)) && \triangleright Z \sim \mathcal{N}(0, 1) \\ &= 1 - \Phi(\Phi^{-1}(1 - \pi)) \\ &= \pi \end{aligned}$$

Thus:

$$\mathbb{P}(f(x_k + r_k + \epsilon; w) = t) \geq \mathbb{P}(x_k + r_k + \epsilon \in \mathcal{A}_k)$$

and based on Lemma A.1, we have:

$$\mathbb{P}(f(x_k + \epsilon; w) = t) \geq \mathbb{P}(x_k + \epsilon \in \mathcal{A}_k) \tag{4}$$

Based on the definition of LDP in Def. 3.3, and for the given samples x_1, \dots, x_k used for LDP computation, we have:

$$\begin{aligned}
s(w) &= \left\| \frac{1}{K} \sum_{k=1}^K \mathbf{p}(x_k|w, \sigma) \right\|_{\infty} \\
&\geq \frac{1}{K} \sum_{k=1}^K p_t(x_k|w, \sigma) \\
&= \frac{1}{K} \sum_{k=1}^K \mathbb{P}(f(x_k + \epsilon; w) = t) &> \text{Def. 3.1} \\
&\geq \frac{1}{K} \sum_{k=1}^K \mathbb{P}(r_k^T(\epsilon - r_k) \geq \sigma \|r_k\|_2 \Phi^{-1}(1 - \pi)) &> \text{Inequality (4)} \\
&= \frac{1}{K} \sum_{k=1}^K \mathbb{P}(Z \geq \Phi^{-1}(1 - \pi) + \frac{\|r_k\|_2}{\sigma}) \\
&\geq \frac{1}{K} \sum_{k=1}^K \mathbb{P}(Z \geq \Phi^{-1}(1 - \pi) + \frac{\Delta}{\sigma}) &> \Delta = \max_{k=1, \dots, K} \|r_k\|_2 \\
&= 1 - \Phi(\Phi^{-1}(1 - \pi) + \frac{\Delta}{\sigma})
\end{aligned}$$

Since the attack is detected if $q_m(w) \leq \alpha$, which is true when $s(w) > s_{(N-m-\lfloor \alpha(N-m+1) \rfloor)}$ is satisfied based on Eq. (2). Thus, the detection of the attack is guaranteed if inequality (3) holds. \square

A.2 Proof of Thm. 4.2

Proof of Thm. 4.2. Let $s_{(1)}, \dots, s_{(N)}$ be the order statistics associated with s_1, \dots, s_N and denote $S = s(W)$ for simplicity. Then, the false positive rate can be represented as the following:

$$\begin{aligned}
&\mathbb{P}(q_m(W) \leq \alpha | \mathcal{S}_N) \\
&= \mathbb{P}(\min\{|\{s \in \mathcal{S}_N : s < S\}|, N - m\} \geq N - m - \alpha(N - m + 1) | \mathcal{S}_N) &> \text{Eq. (2)} \\
&= \mathbb{P}(s_{(N-m)} < S) + \mathbb{P}(s_{(N-m-l)} < S \leq s_{(N-m)}) \\
&= 1 - \tilde{F}(s_{(N-m-l)})
\end{aligned}$$

For any $z \in [0, 1]$, we have:

$$\begin{aligned}
&\mathbb{P}(1 - \tilde{F}(s_{(N-m-l)}) \leq z) \\
&= \mathbb{P}(s_{(N-m-l)} \geq \tilde{F}^{-1}(1 - z)) \\
&\geq \mathbb{P}(s_{(N-m-l)} \geq F^{-1}(1 - z)) &> F \text{ dominates } \tilde{F} \Rightarrow \tilde{F}^{-1} \text{ dominates } F^{-1} \\
&= 1 - \sum_{j=N-m-l}^N \binom{N}{j} (1 - z)^j z^{N-j} &> \text{Distribution of order statistic} \\
&= \sum_{j=0}^{N-m-l-1} \binom{N}{j} (1 - z)^j z^{N-j} &> \text{Binomial expansion} \\
&= I_{(z)}(m + l + 1, N - m - l) &> \text{CDF of Binomial distribution}
\end{aligned}$$

where $I_{(z)}(a, b)$ represents the incomplete Beta function, which is also the CDF of the Beta distribution $\text{Beta}(a, b)$. Thus, the distribution of the false positive rate of our CBD is dominated by a Beta distribution $\text{Beta}(m + l + 1, N - m - l)$ with $l = \lfloor \alpha(N - m + 1) \rfloor$ in the sense of first-order stochastic dominance. \square

A.3 Proof of Col. 4.3

Proof of Col. 4.3. Based on Thm. 4.2, we have

$$\mathbb{P}(Z_N \leq \alpha + (1 - \alpha)\beta + \xi) \geq \mathbb{P}(B \leq \alpha + (1 - \alpha)\beta + \xi) \quad (5)$$

where B follows a Beta distribution $\text{Beta}(m + l + 1, N - m - l)$ with $l = \lfloor \alpha(N - m + 1) \rfloor$. Thus, the mean and variance of B are:

$$\begin{aligned} \mathbb{E}[B] &= \frac{m + l + 1}{N + 1} \\ \text{Var}[B] &= \frac{(m + l + 1)(N - m - l)}{(N + 1)^2(N + 2)} \end{aligned}$$

By Chebyshev's inequality:

$$\mathbb{P}(|B - \frac{m + l + 1}{N + 1}| \geq \xi) \leq \frac{1}{\xi^2} \frac{(m + l + 1)(N - m - l)}{(N + 1)^2(N + 2)} \quad (6)$$

Note that $l = \lfloor \alpha(N - m + 1) \rfloor \in [\alpha(N - m + 1), \alpha(N - m + 1) + 1)$. Thus, algebra shows that:

$$\begin{aligned} &\mathbb{P}(B \geq \alpha + (1 - \alpha)\beta + \xi + \frac{\alpha + 1}{N}) \\ &= \mathbb{P}(B \geq \frac{m + \alpha(N - m + 1) + 1}{N} + \xi) \\ &\leq \mathbb{P}(B \geq \frac{m + l + 1}{N + 1} + \xi) \\ &\leq \mathbb{P}(|B - \frac{m + l + 1}{N + 1}| \geq \xi) \end{aligned}$$

and

$$\begin{aligned} &\frac{1}{\xi^2(N + 2)} (\beta + \alpha(1 - \beta + \frac{1}{N}) + \frac{1}{N})(1 - \beta - \alpha(1 - \beta + \frac{1}{N}) + \frac{1}{N}) \\ &= \frac{1}{\xi^2} \frac{(m + \alpha(N - m + 1) + 1)(N - m - \alpha(N - m + 1) + 1)}{N^2(N + 2)} \\ &\geq \frac{1}{\xi^2} \frac{(m + l + 1)(N - m - l)}{(N + 1)^2(N + 2)} \end{aligned}$$

According to inequality (6) and also because of the continuity of the Beta distribution:

$$\begin{aligned} &\lim_{N \rightarrow +\infty} \mathbb{P}(B \leq \alpha + (1 - \alpha)\beta + \xi) \\ &= \lim_{N \rightarrow +\infty} \mathbb{P}(B \leq \alpha + (1 - \alpha)\beta + \xi + \frac{\alpha + 1}{N}) \\ &= 1 - \lim_{N \rightarrow +\infty} \mathbb{P}(B \geq \alpha + (1 - \alpha)\beta + \xi + \frac{\alpha + 1}{N}) \\ &\geq 1 - \lim_{N \rightarrow +\infty} \frac{1}{\xi^2(N + 2)} (\beta + \alpha(1 - \beta + \frac{1}{N}) + \frac{1}{N})(1 - \beta - \alpha(1 - \beta + \frac{1}{N}) + \frac{1}{N}) \\ &= 1 \end{aligned}$$

Thus, the corollary is proved by applying the sandwich theorem to inequality (5). \square

B Stochastic Dominance Assumption in Thm. 4.2

In Thm. 4.2, we assume that the distribution F for the LDP of the benign shadow models with inadequate training dominates the distribution \tilde{F} for the LDP of the actual benign classifiers trained on more abundant data in the sense of first-order stochastic dominance. This assumption holds in general in practice. It is widely believed that models are trained to learn the data distribution [26]. Thus, intuitively, training with insufficient sampling of the data distribution will not only lead to

a high empirical loss but also result in a poor robustness on the test instances. In our setting, this is reflected by a small samplewise local probability for the labeled class for most samples used for computing LDP, which may easily lead to a large LDP. In the following, we show that a larger deviation of the learned decision boundary of a binary Bayesian classifier will affect its LDP. The analysis can be extended to multi-class scenarios based on the “winner takes all” rule. Some notations may be abused but are all constrained to the current section.

Theorem B.1. *Consider two classes $\{a, b\}$ with equal prior and arbitrary sample distributions μ_a and μ_b , respectively. Consider a Bayes classifier $g(z) = \arg \max_{k \in \{a, b\}} \mu_k(z)$ (i.e. with a decision boundary $\frac{\mu_a(z)}{\mu_b(z)} = 1$). We arbitrarily assume that the expected LDP for g is associated with class b :*

$$s = \frac{1}{2}(\mathbb{E}_{X \sim \mu_a}[\mathbb{P}(g(X + \epsilon) = b)] + \mathbb{E}_{X \sim \mu_b}[\mathbb{P}(g(X + \epsilon) = b)]) \quad (7)$$

Moreover, consider any two classifiers g_1 and g_2 with decision boundaries $\frac{\mu_a(z)}{\mu_b(z)} = t_1$ and $\frac{\mu_a(z)}{\mu_b(z)} = t_2$, respectively. Then, if $t_2 \geq t_1 \geq 1$, the expected LDP for the two classifiers, denoted by s_1 and s_2 , respectively, will satisfy $s_2 \geq s_1 \geq s$, i.e. the more deviation in the decision boundary from the optimum, the larger expected LDP.

Proof. For each $i \in \{1, 2\}$, the expectation of the LDP for classifier g_i can be expressed as:

$$s_i = \max_{k \in \{a, b\}} \frac{1}{2}(\mathbb{E}_{X \sim \mu_a}[g_i(X + \epsilon) = k] + \mathbb{E}_{X \sim \mu_b}[g_i(X + \epsilon) = k]) \quad (8)$$

Since $t_2 \geq t_1 \geq 0$, given the decision boundaries of g_1 and g_2 , we have:

$$\begin{aligned} & \mathbb{E}_{X \sim \mu_a}[\mathbb{P}(g_1(X + \epsilon) = a)] \\ &= \int \mathbb{P}\left(\frac{\mu_a(z + \epsilon)}{\mu_b(z + \epsilon)} > t_1\right) \mu_a(z) dz \\ &= \int \left[\mathbb{P}\left(\frac{\mu_a(z + \epsilon)}{\mu_b(z + \epsilon)} > t_2\right) + \mathbb{P}\left(t_1 < \frac{\mu_a(z + \epsilon)}{\mu_b(z + \epsilon)} \leq t_2\right) \right] \mu_a(z) dz \\ &= \mathbb{E}_{X \sim \mu_a}[\mathbb{P}(g_2(X + \epsilon) = a)] + \int \mathbb{P}\left(t_1 < \frac{\mu_a(z + \epsilon)}{\mu_b(z + \epsilon)} \leq t_2\right) \mu_a(z) dz \end{aligned}$$

and similarly,

$$\begin{aligned} & \mathbb{E}_{X \sim \mu_b}[\mathbb{P}(g_2(X + \epsilon) = b)] \\ &= \int \mathbb{P}\left(\frac{\mu_a(z + \epsilon)}{\mu_b(z + \epsilon)} \leq t_2\right) \mu_b(z) dz \\ &= \int \left[\mathbb{P}\left(\frac{\mu_a(z + \epsilon)}{\mu_b(z + \epsilon)} \leq t_1\right) + \mathbb{P}\left(t_1 < \frac{\mu_a(z + \epsilon)}{\mu_b(z + \epsilon)} \leq t_2\right) \right] \mu_b(z) dz \\ &= \mathbb{E}_{X \sim \mu_b}[\mathbb{P}(g_1(X + \epsilon) = b)] + \int \mathbb{P}\left(t_1 < \frac{\mu_a(z + \epsilon)}{\mu_b(z + \epsilon)} \leq t_2\right) \mu_b(z) dz \end{aligned}$$

According to above relations between g_1 and g_2 , we have

$$\begin{aligned} & \frac{1}{2}(\mathbb{E}_{X \sim \mu_a}[\mathbb{P}(g_2(X + \epsilon) = b)] + \mathbb{E}_{X \sim \mu_b}[\mathbb{P}(g_2(X + \epsilon) = b)]) \\ &= \frac{1}{2}(1 - \mathbb{E}_{X \sim \mu_a}[\mathbb{P}(g_2(X + \epsilon) = a)] + \mathbb{E}_{X \sim \mu_b}[\mathbb{P}(g_2(X + \epsilon) = b)]) \\ &= \frac{1}{2}\left(1 - \mathbb{E}_{X \sim \mu_a}[\mathbb{P}(g_1(X + \epsilon) = a)] + \int \mathbb{P}\left(t_1 < \frac{\mu_a(z + \epsilon)}{\mu_b(z + \epsilon)} \leq t_2\right) \mu_a(z) dz \right. \\ & \quad \left. + \mathbb{E}_{X \sim \mu_b}[\mathbb{P}(g_1(X + \epsilon) = b)] + \int \mathbb{P}\left(t_1 < \frac{\mu_a(z + \epsilon)}{\mu_b(z + \epsilon)} \leq t_2\right) \mu_b(z) dz\right) \\ &= \frac{1}{2}(\mathbb{E}_{X \sim \mu_a}[\mathbb{P}(g_1(X + \epsilon) = b)] + \mathbb{E}_{X \sim \mu_b}[\mathbb{P}(g_1(X + \epsilon) = b)]) \\ & \quad + \frac{1}{2} \int \mathbb{P}\left(t_1 < \frac{\mu_a(z + \epsilon)}{\mu_b(z + \epsilon)} \leq t_2\right) (\mu_a(z) + \mu_b(z)) dz \\ &\geq \frac{1}{2}(\mathbb{E}_{X \sim \mu_a}[\mathbb{P}(g_1(X + \epsilon) = b)] + \mathbb{E}_{X \sim \mu_b}[\mathbb{P}(g_1(X + \epsilon) = b)]) \end{aligned}$$

Similarly, since $t_1 \geq 1$, for g_1 and g , we have:

$$\begin{aligned} & \frac{1}{2} (\mathbb{E}_{X \sim \mu_a} [\mathbb{P}(g_1(X + \epsilon) = b)] + \mathbb{E}_{X \sim \mu_b} [\mathbb{P}(g_1(X + \epsilon) = b)]) \\ & \geq \frac{1}{2} (\mathbb{E}_{X \sim \mu_a} [\mathbb{P}(g(X + \epsilon) = b)] + \mathbb{E}_{X \sim \mu_b} [\mathbb{P}(g(X + \epsilon) = b)]) \end{aligned}$$

Thus, $s_2 \geq s_1 \geq s$ if $t_2 \geq t_1 \geq 1$. □

C Details for the Experimental Setup

C.1 Details for the Datasets

GTSRB is an image dataset for German traffic signs from 43 classes [60]. The training set and the test set contain 39,209 and 12,630 images, respectively. The image sizes vary in a relatively large range. Thus, we resize all the images to 32×32 in our experiments for convenience.

SVHN is a real-world image dataset created from house numbers in Google Street View images. It contains 32×32 color images from the 10 classes of the ten digits [47]. The training set and the test set contain 73,257 and 26,032 images, respectively.

CIFAR-10 is a benchmark dataset with 32×32 color images from 10 classes for different categories of objects [30]. The training set contains 50,000 images, and the test set contains 10,000 images, both evenly distributed in the 10 classes.

TinyImageNet is a subset of the ImageNet dataset [11]. It contains color images from 200 classes downsized to 64×64 . The training set and the test set contain 100,000 and 10,000 images, respectively, both evenly distributed into the 200 classes.

C.2 Details for Trigger Generation in Sec. 5.1.1

The triggers used by the attacks to evaluate the certification of CBD are generated with randomness. But for each attack, once the trigger is generated, the same trigger will be used by all the poisoned images. For the trigger pattern on GTSRB, each pixel is randomly perturbed with a 0.25 probability. For each pixel being perturbed, the perturbation sizes for all three channels are randomly and independently selected in the interval $[0, 12/255]$. For the trigger pattern on SVHN, each pixel among the 16×16 patch on the top left of the image is randomly perturbed with a 0.5 probability. The perturb sizes for all three channels are randomly and independently selected between $-9/255$ and $9/255$. For the trigger pattern on CIFAR-10, we found that purely random patterns are too hard to learn, even with the help of nullification. Thus, we use the recursive pattern that looks like a chessboard in [75], but with the perturbation size randomly selected from $1/255$, $2/255$, $3/255$, and $4/255$. For TinyImageNet, we used the same trigger generation approach as for SVHN. For all the patterns, we apply a projection to ensure that the ℓ_2 norm of the trigger perturbation is no larger than 0.75.

C.3 Detailed Training Configurations

For GTSRB, training is performed for 100 epochs with a batch size of 128 and a learning rate of 10^{-3} (with 0.1 decay per 20 epochs), using the Adam optimizer [28]. Each training image is also augmented with a ± 5 degree random rotation.

For SVHN, training is performed for 50 epochs with a batch size of 128 and a learning rate of 10^{-3} , also using the Adam optimizer. Each training image is augmented with a random horizontal flipping.

For CIFAR-10, training is performed for 100 epochs with a batch size of 32 and a learning rate of 10^{-3} , using the Adam optimizer. Training data augmentation involves random horizontal flipping and random cropping.

For TinyImageNet, training is performed for 100 epochs with a batch size of 128 and a learning rate of 10^{-3} , using the Adam optimizer. Training data augmentation involves random horizontal flipping and random cropping.

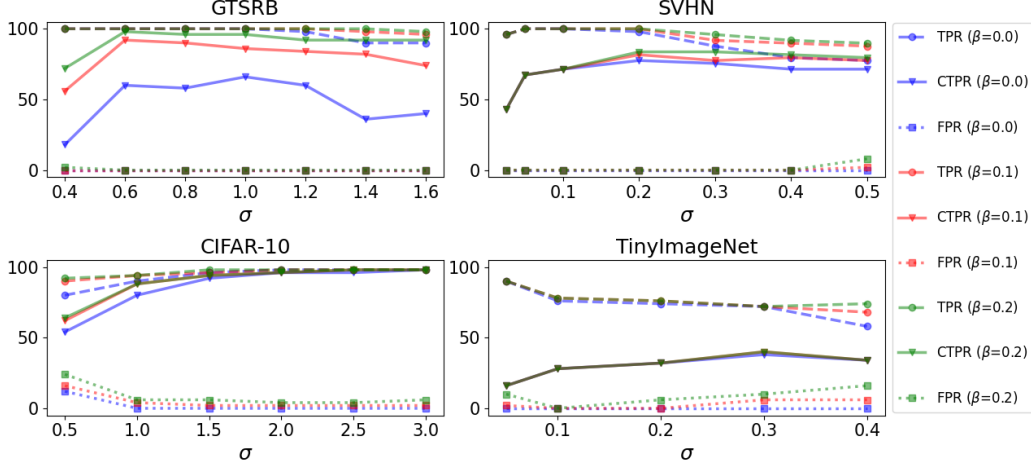


Figure 5: CTPR (solid) of CBD against backdoor attacks with random perturbation triggers with perturbation magnitude $\ell_2 \leq 0.75$ over a range of σ for $\beta = m/N \in \{0, 0.1, 0.2\}$ for the four datasets. TPR (dashed) and FPR (dotted) are also plotted for reference.

C.4 Details for the Triggers Uses in Sec. 5.2

For the BadNet trigger in [18], we use a 2×2 noisy patch with a randomly selected location for each attack on GTSRB and CIFAR-10. For SVHN, we increase the patch size to 3×3 to ensure the trigger is learned. The poisoning ratios on GTSRB, SVHN, and CIFAR-10 are 7.8%, 0.4%, and 3%, respectively.

For the “chessboard” pattern in [75], we use 3/255 maximum perturbation magnitude for SVHN and CIFAR-10. For GTSRB, we use a larger perturbation magnitude 6/255 to ensure the trigger is learned. The poisoning ratios on GTSRB, SVHN, and CIFAR-10 are 7.8%, 2.7%, and 6%, respectively.

For the blend trigger in [8], we generate an image-wide noisy pattern as the trigger, with a mixing rate of 0.1. The poisoning ratios on GTSRB, SVHN, and CIFAR-10 are 7.8%, 2.7%, and 3%, respectively.

D Additional Certification Results

In Sec. 5.1, we focused on backdoor attacks with random perturbation triggers with perturbation magnitude $\ell_2 \leq 0.75$. In Fig. 2, we showed the CTPR and TPR for CBD to validate our detection guarantee on backdoored models. In particular, we showed that CBD achieves maximum CTPRs (TPRs) 98% (100%), 84% (100%), 98% (98%), and 40% (72%) on GTSRB, SVHN, CIFAR-10, and TinyImageNet, respectively, across all choices of σ and β . Here, in Fig. 5, we also show the FPR for all combinations of σ and β . Especially, the FPRs corresponding to the aforementioned TPRs and CTPRs on the four datasets are 0%, 0%, 6%, and 10%, respectively. From the figure, we also observe that for $\beta \leq 0.2$, CTPR and/or TPR may be improved by the increment in β , with a rather small sacrifice in FPR.

Also, in this section, we consider triggers with larger perturbation magnitudes with $0.75 < \ell_2 \leq 1.5$. The experiments follow the same settings as described in Sec. 5.1.1. The ℓ_2 constraint is satisfied by increasing the per-pixel perturbation sizes accordingly. For GTSRB, for example, the trigger is generated in the same way as described in App. C.2, but for each pixel being perturbed, the perturbation sizes for all three channels are randomly and independently selected in the interval $[12/255, 24/255]$. In Fig. 6, we show the CTPR for the same range of σ for each dataset as in Fig. 5, and for $\beta = 0, 0.1, 0.2$. The TPR and the FPR are also plotted for reference. Compared with the performance of CBD for triggers with smaller perturbation magnitudes, there is a drop in both CTPR and TPR, especially for GTSRB and SVHN. However, CBD still achieves up to 100% (68%), 100% (76%), 100% (100%), and 84% (28%) empirical (certified) true positive rates on GTSRB, SVHN, CIFAR-10, and TinyImageNet, respectively.

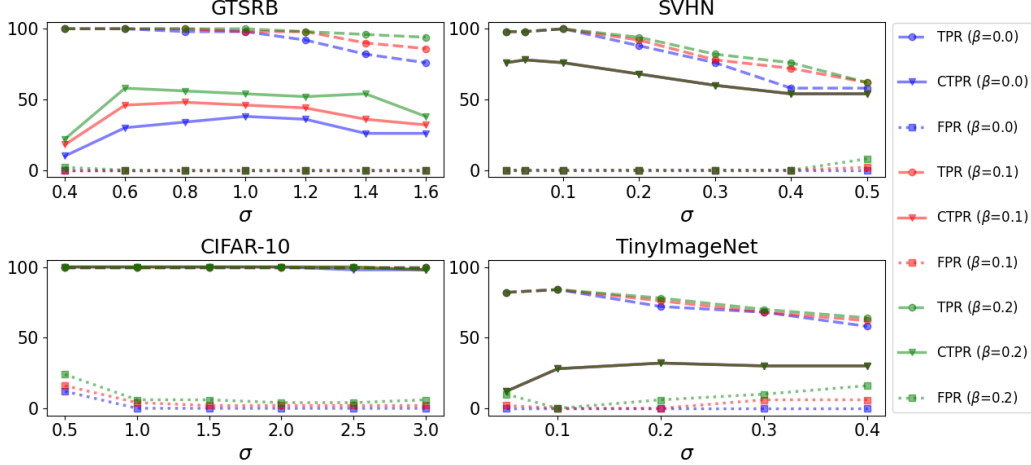


Figure 6: CTPR (solid) of CBD against backdoor attacks with random triggers with perturbation magnitude $0.75 < \ell_2 \leq 1.5$ over a range of σ for $\beta = m/N \in \{0, 0.1, 0.2\}$ for the four datasets. TPR (dashed) and FPR (dotted) are also plotted for reference.

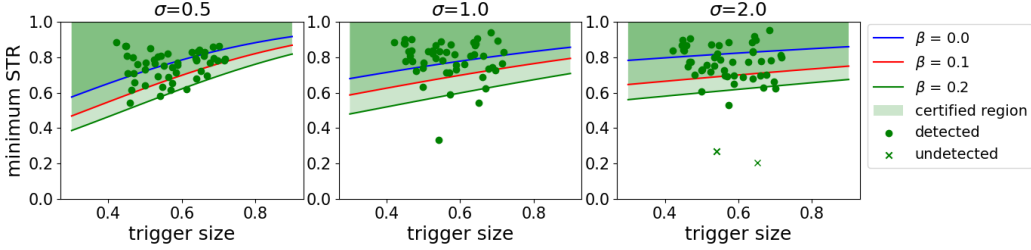


Figure 7: Example of the certified region obtained using Thm. 4.1 on GTSRB. Most of the attacks with random triggers with magnitude constraint $\ell_2 \leq 0.75$ fall into the certified region for $\beta = 0.2$.

In Fig. 7 and Fig. 8, we show the example certified regions on GTSRB for $\sigma = 0.5, 1.0, 2.0$ and for $\beta = 0, 1.0, 2.0$. The certified regions in the two sets of figures are obtained from Thm. 4.1 though plotted for different ranges of the trigger size. For all combinations of σ and β , the shape of the certified region matches our theoretical result that attacks with a larger STR and a smaller perturbation size of the trigger are more likely to be detected with a guarantee. Especially for a larger trigger size, the detection guarantee also requires a larger STR, resulting in a reduced margin for the certified region as the trigger size grows.

In Fig. 7, we show that empirically, most of the attacks with the random perturbation trigger satisfying the $\ell_2 \leq 0.75$ constraint fall into the certified region associated with $\beta = 0.2$, showing the strong detection and certification power of our CBD against attacks with moderate-sized triggers. In Fig. 8, for larger trigger perturbation magnitudes, there is a drop in the number of attacks falling into the certified region, leading to a drop in the CTPR. Although these results show the limitation of CBD certification against triggers with overly large perturbation magnitudes, these triggers may be easily revealed by other (even simpler) detectors, including a human inspection. Moreover, we found that sometimes, the minimum STR of an attack increases as the perturbation magnitude of the trigger increases. The same phenomenon is also observed on CIFAR-10, which allows attacks with even larger trigger perturbation magnitudes to be detected and certified by our CBD. One possible reason is that for triggers with a small perturbation magnitude, the class discriminate features in the samples embedded with the trigger may compromise the learning of the trigger during training.

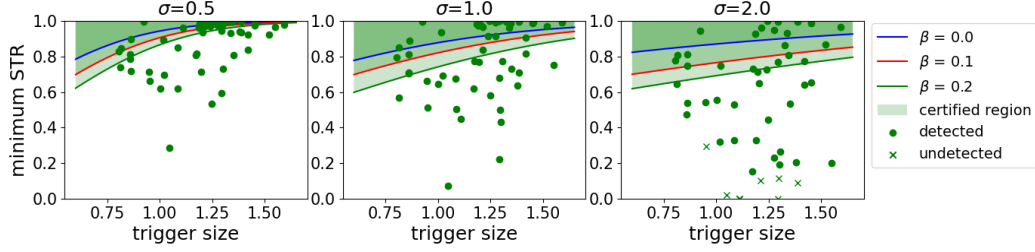


Figure 8: Example of the certified region obtained using Thm. 4.1 on GTSRB (plotted for a different range of trigger sizes compared with Fig. 7). There are still many attacks with random triggers with magnitude constraint $0.75 < \ell_2 \leq 1.5$ fall into the certified region.

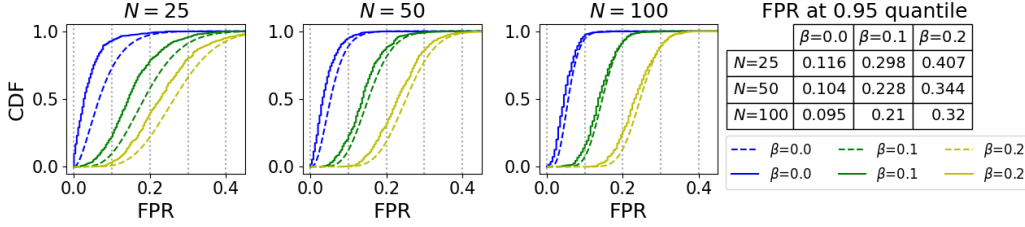


Figure 9: Validation of the FPR upper bound in Thm. 4.2 using the shadow models on GTSRB. For each calibration size N and β , the empirical CDF of the FPR (solid) is indeed dominated by the CDF of the Beta random variable (dashed) derived by Thm. 4.2. In the table on the right, the decrement of FPR at 0.95 quantiles as N grows implies a better FPR control with a larger calibration set.

E Empirical Validation of the FPR Guarantee

We validate the probabilistic upper bound for the FPR in Thm. 4.2 using the shadow models on GTSRB as an example. We train 300 shadow models and sample a number of them to form the calibration set to evaluate the FPR on the remaining ones. Such a process is repeated 500 times for each calibration size $N \in \{25, 50, 100\}$ and $\beta = m/N \in \{0, 0.1, 0.2\}$, which produces an empirical CDF for each combination of N and β , as shown in Fig. 9. Since in the settings here, the LDP distribution for the classifiers to be inspected is the same as the distribution of the LDPs in the calibration set, the stochastic dominance assumption in Thm. 4.2 is satisfied. Thus, for each N and β , the empirical CDF (solid) is dominated by the CDF of the Beta random variable obtained by Thm. 4.2 (dashed) as shown in Fig. 9. Moreover, we find that for all β choices, the FPR value at 0.95 quantile decreases as N increases, which implies that a larger calibration set (which requires more shadow models) may help to reduce the worst cases FPR.

F Computational Complexity

For a new domain, our detection procedure requires N shadow model training and $(N + 1)$ LDP estimation. The N shadow models and their estimated LDP statistics can also be used in the future for the same domain. On a single RTX 2080 Ti card, training of one shadow model on GTSRB, SVHN, CIFAR-10, and TinyImageNet requires 39s, 45s, 31s, and 2462s, respectively, while LDP estimation requires 8s, 4s, 7s, and 86s on the four datasets respectively.

G Additional Technical Details for CBD Detection and Certification

In Sec. 3.4, we described the detection procedure of CBD, which employs an adjustable conformal prediction that assumes m overly large outliers in the calibration set, where m may be prescribed based on prior knowledge. Here, we introduce a simple scheme based on anomaly detection that can be used to determine m in practice with very little prior knowledge. Let $\mathcal{S}_N = \{s_1, \dots, s_N\}$ be the calibration set of LDP statistics obtained from the shadow models. Our goal is to check if there are

large outliers. To this end, we compute the median absolute deviation (MAD [21]) over the elements in \mathcal{S}_N by $\text{MAD} = \text{median}_{s \in \mathcal{S}_N}(|s - \text{median}_{s' \in \mathcal{S}_N}(s')|)$. Under the Gaussian assumption, an outlier s for 0.05 single-tailed significance level will satisfy $(s - \text{median}_{s' \in \mathcal{S}_N}(s')) / (1.4826 \cdot \text{MAD}) \geq 1.645$. Using this scheme, we obtain the proportion of outliers $\beta = m/N$ as 0.16, 0.03, 0.01, and 0.06 for GTSRB, SVHN, CIFAR-10, and TinyImageNet, respectively. While the scheme suggests relatively conservative adjustment to the conformal prediction for most datasets, the suggested choice of β for GTSRB will lead to a clear increment in CTPR with negligible increment in FPR, based on our results in Fig. 5. Other anomaly detection methods with more prior knowledge may also be used.

In this section, we also present the detailed algorithm for CBD detection and certification.

Algorithm 1 Algorithm for CBD detection

- 1: **Input:** classifier $f(\cdot; w)$ to be inspected with K classes; clean validation set \mathcal{D} for detection.
 - 2: **Hyperparameter:** standard deviation σ for the Gaussian noise; size of the calibration set N ; number of assumed outliers in the calibration set m ; significance level α for conformal prediction; J random samples of the Gaussian noise ($J = 1024$ in our experiments).
 - 3: **Step 1: estimate LDP for $f(\cdot; w)$.**
 - 4: Randomly sample x_1, \dots, x_K from \mathcal{D} satisfying $f(x_k; w) = k$ for $\forall k \in \{1, \dots, K\}$.
 - 5: **for** $k = 1 : K$ **do**
 - 6: Initialize a frequency vector $\mathbf{q} = \mathbf{0}$
 - 7: **for** $j = 1 : J$ **do**
 - 8: Sample ϵ from $\mathcal{N}(0, \sigma^2 I)$
 - 9: Get the class decision $y = f(x_k + \epsilon; w)$
 - 10: $[\mathbf{q}]_y \leftarrow [\mathbf{q}]_y + 1$
 - 11: Compute SLPV for x_k by: $\mathbf{p}(x_k|w, \sigma) = \frac{\mathbf{q}}{\|\mathbf{q}\|_1}$
 - 12: Compute LDP for $f(\cdot; w)$ by: $s(w) = \|\frac{1}{K} \sum_{k=1}^K \mathbf{p}(x_k|w, \sigma)\|_\infty$
 - 13: **Step 2: construct a calibration set \mathcal{S}_N .**
 - 14: Train shadow models $f(\cdot; w_1), \dots, f(\cdot; w_N)$ on randomly sampled $\mathcal{D}_{\text{Train}} \subset \mathcal{D}$
 - 15: **for** $n = 1 : N$ **do**
 - 16: Randomly sample $x_1^{(n)}, \dots, x_K^{(n)}$ from $\mathcal{D} \setminus \mathcal{D}_{\text{Train}}$ satisfying $f(x_k^{(n)}; w_n) = k$ for $\forall k \in \{1, \dots, K\}$.
 - 17: **for** $k = 1 : K$ **do**
 - 18: Initialize a frequency vector $\mathbf{q} = \mathbf{0}$
 - 19: **for** $j = 1 : J$ **do**
 - 20: Sample ϵ from $\mathcal{N}(0, \sigma^2 I)$
 - 21: Get the class decision $y = f(x_k^{(n)} + \epsilon; w_n)$
 - 22: $[\mathbf{q}]_y \leftarrow [\mathbf{q}]_y + 1$
 - 23: Compute SLPV for $x_k^{(n)}$ by: $\mathbf{p}(x_k^{(n)}|w_n, \sigma) = \frac{\mathbf{q}}{\|\mathbf{q}\|_1}$
 - 24: Compute LDP for $f(\cdot; w_n)$ by: $s(w_n) = \|\frac{1}{K} \sum_{k=1}^K \mathbf{p}(x_k^{(n)}|w_n, \sigma)\|_\infty$
 - 25: Construct calibration set $\mathcal{S}_N = \{s(w_1), \dots, s(w_N)\}$.
 - 26: **Step 3&4: adjustable conformal prediction.**
 - 27: Compute p-value $q_m(w) = 1 - \frac{1 + \min\{|\{s \in \mathcal{S}_N : s \leq s(w)\}|, N - m\}}{N - m + 1}$.
 - 28: **Output:** $f(\cdot; w)$ is backdoored if $q_m(w) \leq \alpha$; otherwise, $f(\cdot; w)$ is not backdoored.
-

H Effectiveness of Backdoor Attacks with Random Perturbation Trigger

In Sec. 5.1, we evaluated the certification performance of our CBD against backdoor attacks with the random perturbation trigger. The attacks were implemented following the conventional strategy by poisoning the training set with some images embedded with the trigger and labeled to the backdoor target class. We stated that attacks with poisoning rate lower than those used by our experiments will easily lead to a failed attack.

Here, we show more details regarding the effectiveness of these attacks. In particular, we focus on the CIFAR-10 dataset as an example. In Sec. 5.1, we used a 11.3% poisoning rate (250 poisoned images from 9 classes other than the backdoor target class, divided by 20000 training images). Here, we also consider attacks with 50, 100, 150, and 200 poisoned images per class, i.e. with 2.3%, 4.5%,

Algorithm 2 Algorithm for CBD Certification

- 1: **Input:** backdoor trigger δ ; target class t ; victim classifier $f(\cdot; w)$ with K classes; samples x_1, \dots, x_K for detection; calibration set \mathcal{S}_N ; a standard Gaussian CDF Φ .
 - 2: **Hyperparameter:** standard deviation σ for the Gaussian noise; size of the calibration set N ; number of assumed outliers in the calibration set m ; significance level α for conformal prediction; J random samples of the Gaussian noise ($J = 1024$ in our experiments).
 - 3: **for** $k = 1 : K$ **do**
 - 4: Initialize $r = 0$
 - 5: **for** $j = 1 : J$ **do**
 - 6: Sample ϵ from $\mathcal{N}(0, \sigma^2 I)$
 - 7: **if** $f(\delta(x_k) + \epsilon; w) = t$ **then**
 - 8: $r \leftarrow r + 1$
 - 9: STR for x_k is $R_{\delta,t}(x_k|w, \sigma) = \frac{r}{J}$.
 - 10: $\pi = \min_{k=1, \dots, K} R_{\delta,t}(x_k|w, \sigma)$.
 - 11: $\Delta = \max_{k=1, \dots, K} \|\delta(x_k) - x_k\|_2$.
 - 12: Get $S = s_{(N-m-\lfloor \alpha(N-m+1) \rfloor)}$ from the calibration set \mathcal{S}_N .
 - 13: **Output:** If $\Delta < \sigma(\Phi^{-1}(1-S) - \Phi^{-1}(1-\pi))$, the attack is guaranteed to be detected; otherwise, the attack may be detected but without guarantee.
-

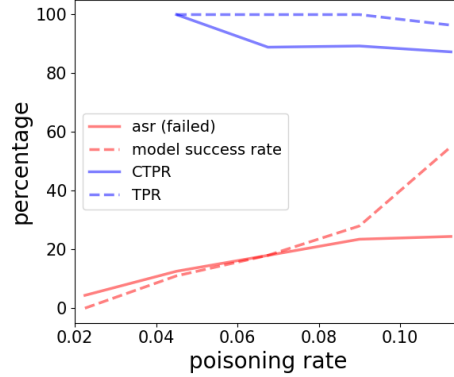


Figure 10: Analysis of the effectiveness of the backdoor attacks with the random perturbation trigger on CIFAR-10. CBD is effective in both detection and certification for a range of poisoning rates.

6.8%, and 9% poisoning rates, respectively. For each poisoning rate, we create 100 attacks and train one model for each attack. The backdoor target class for each attack is randomly selected.

In Fig. 10, we show for each poisoning rate the *model success rate*, which is the proportion of attacks with the (samplewise) attack success rate no less than 90%. We also show the average (samplewise) attack success rate for all the failed attacks for each poisoning rate. With low poisoning rates, the attack may easily fail. But as long as an attack is successful, our CBD is able to detect it with high accuracy, possibly with a guarantee as well.

I Difference Between Certified Backdoor Detection and Certified Robustness Against Adversarial Examples

The certification for backdoor detection is fundamentally different from the certification for robustness against adversarial examples from the following five aspects:

- The strength and the stealthiness of an adversarial example are both determined by the adversarial perturbation size. However, for a successful backdoor attack (failed attacks are not supposed to be detected or certified), the attack strength is determined by the robustness of the learned trigger, while the stealthiness is determined by the trigger perturbation magnitude. Thus, for adversarial

examples, a 1-D interval specified by the *certified radius* is derived, while for our CBD, we derive a 2-D *certified region* jointly specified by the trigger robustness and its perturbation magnitude.

- Certification for adversarial examples by randomized smoothing investigates the decision region near a given input. Differently, our certification method for backdoor detection focuses on the model behavior instead, since we are detecting backdoored models. Such model behavior is quantified by our proposed LDP statistic computed on a set of samples from all classes (Definition 3.3).
- Certification for adversarial examples is uni-directional, which provides guarantees on desired model predictions. By contrast, our certification for backdoored model detection is bi-directional. We not only provide guarantees on the detection of backdoored models but also control the false detection rate on benign models. Otherwise, one can easily design a backdoor detector that always triggers an alarm, which provides detection guarantees to all backdoor attacks but is useless in practice.
- For both adversarial examples and backdoor attacks, certified robustness and certified detection have different adversarial constraints – they cover the two ends of the attack strength, respectively. For adversarial examples, existing certifications are all robustness guarantees that cover weak adversarial attacks with small perturbation magnitudes. For backdoor attacks, existing certified defenses provide robustness guarantees on the training-time failure of trigger injection into the model and/or test-time failure of trigger recognition – both failures require the attack to be sufficiently weak. Our CBD, however, focuses on certified backdoor detection, which addresses strong backdoor attacks with robust triggers.
- A strong certified robustness against adversarial examples (and also backdoor attacks) is usually achieved by robust training, which requires the defender to have full access to the training process. However, our certified backdoor detector is deployed post-training, which allows the attacker to have full control of the training process.